IGARSS 2014

Recent Advances in Registration, Integration and Fusion of Remotely Sensed Data: Redundant Representations and Frames

Wojciech Czaja[1] and Jacqueline Le Moigne[2]

July 13, 2014

1. *University of Maryland, Norbert Wiener Center for Harmonic Analysis and Applications*
2. *NASA Goddard Space Flight Center, Software Engineering Division*

Section 1
Introduction to registration, integration and fusion of remotely sensed data

Section 1a
Overview of issues and challenges

Image Registration in the Context of Space Missions

Image Registration in the Context of Space Missions

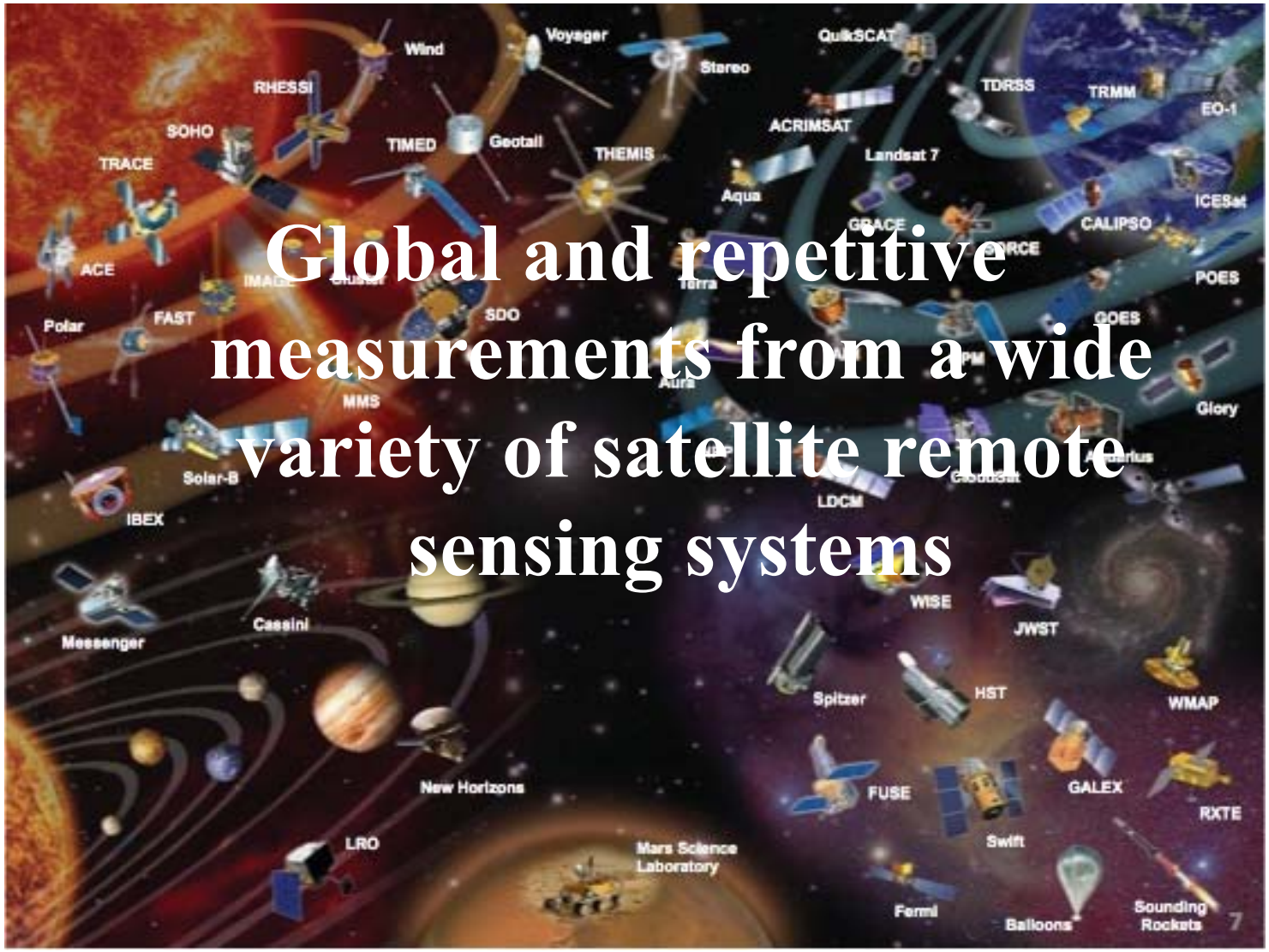

Image Registration in the Context of Earth Remote Sensing

Example of Various Spatial and Spectral Characteristics

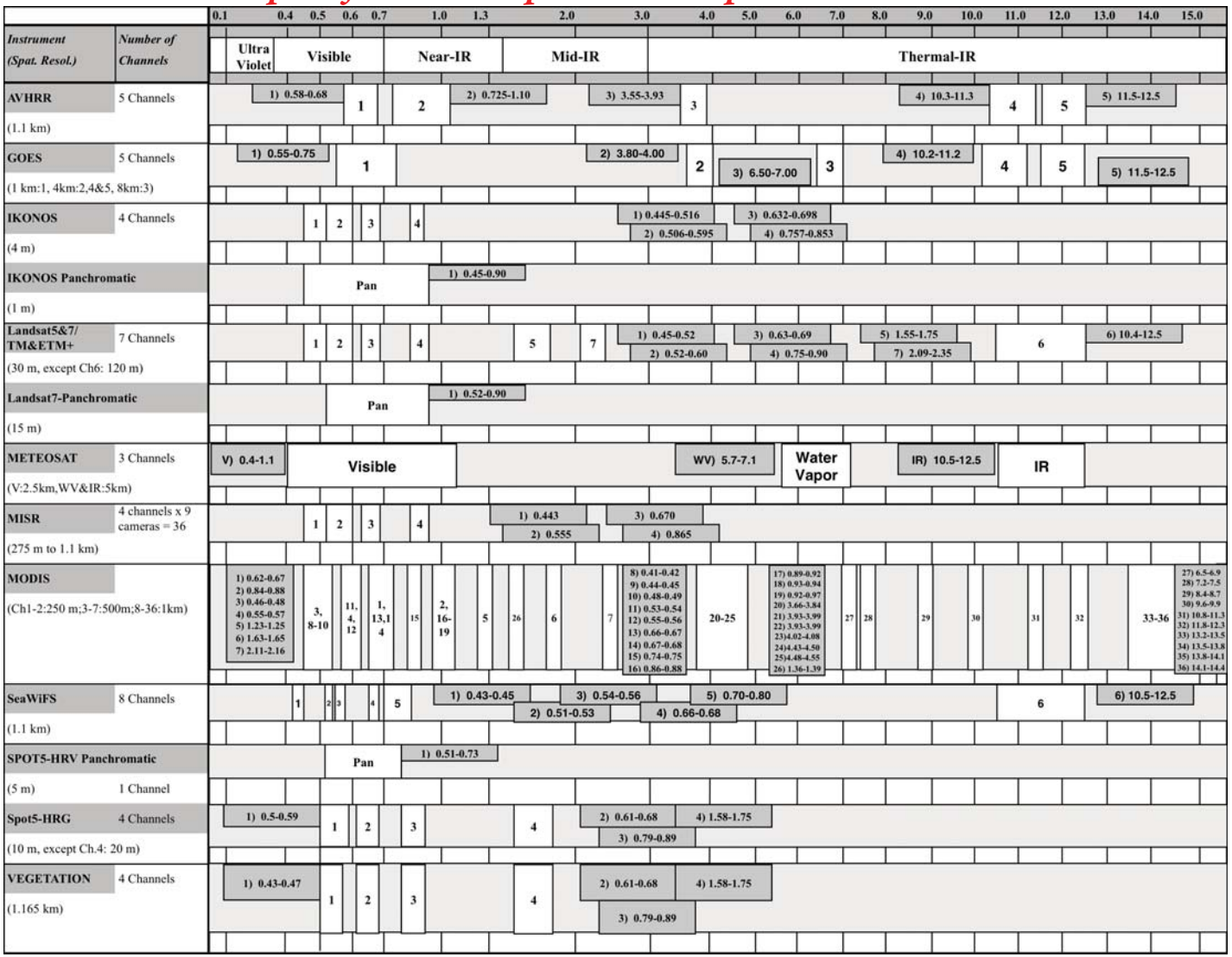

What is Image Registration …

- Definition

  "Exact pixel-to-pixel matching of two different images or matching of one image to a map"

- Navigation or Model-Based Systematic Correction
  - Orbital, Attitude, Platform/Sensor Geometric Relationship, Sensor Characteristics, Earth Model, etc.
- Image Registration/Feature-Based Precision Correction
  - Navigation within a Few Pixels Accuracy
  - Image Registration Using Selected Features (or Control Points) to Refine Geo-Location Accuracy
- Image Registration as a Post-Processing or as a Feedback to Navigation Model

What is Data Integration and Fusion …

- Definition "Data Integration"

  "*Data integration means combining data coming from different sources and providing users with a unified view of these data*"

  - It usually does not refer to the extraction of relevant information, but rather to combination and/or concatenation of data (e.g. for a GIS or data assimilation or within a model)

- Definition "Data Fusion"

  "*Data fusion is a formal framework in which are expressed the means and tools for the alliance of data originating from different sources. Data fusion aims at obtaining information of greater quality; the exact definition of 'greater quality' will depend upon the application.*" (Wald, 1999)

The Role of Image Registration and Fusion in the Processing of Remotely Sensed Data

- Essential for spatial and radiometric calibration of multitemporal measurements for creating long-term phenomenon tracking data

- Used for accurate change detection and land cover/ land use assessment

- Basis for extrapolating data throughout several scales for multi-scale phenomena (distinguish between natural and human-induced)

Impact of Misregistration

- (Towsnhend et al, 1992) and (Dai & Khorram, 1998): small error in registration may have a large impact on global change measurements accuracy
- e.g., 1 pixel misregistration error => 50% error in Vegetation Index (NDVI) computation (using 250m MODIS data)

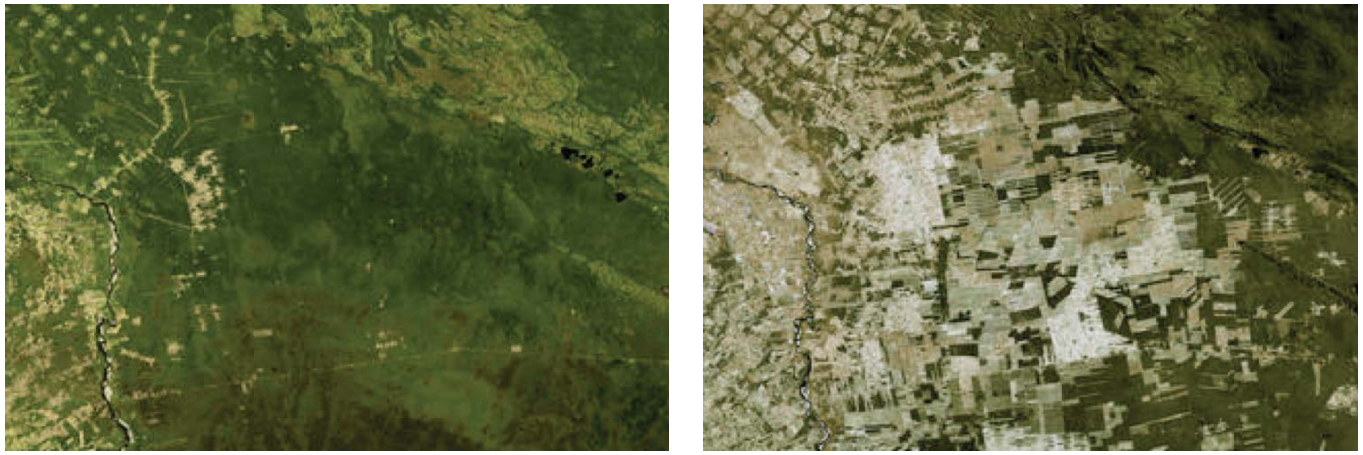

Human-induced land cover changes observed by Landsat-5 in Bolivia in 1984 and 1998 (Courtesy: Compton J. Tucker and the Landsat Project, NASA Goddard Space Flight Center)

- Influence of image registration on products validation
- Impact of misregistration on legal, economic and sociopolitical (e.g., resource management), etc.

Image Registration and Fusion Applications

- *Multimodal registration and fusion,* for integrating complementary information from multiple sensors
  - Example: LIDAR and optical data for precision landing
- *Multitemporal registration and integration,* for change detection and Earth resource surveying
  - Example: Landsat Program, Landsat-4/5, Landsat-7 and Landsat-8
- *Viewpoint registration and fusion,* for landmark navigation, formation flying (sensor web) and planet exploration
  - Example: Landsat-7, EO-1 and MODIS for disaster management
- *Template registration and integration,* for content-based searching or map updating
  - Example: Finding flux towers in MODIS or EO-1 data

Challenges in Image Registration for Remote Sensing

- Remote Sensing vs. Medical or Other Imagery ("Big Data")
  - Variety in the types of sensor data and the conditions of data acquisition
  - Size of the data
  - Lack of a known image model
  - Lack of well-distributed "fiducial points"
- Navigation Error (or varying "Initial Conditions")
  - Historical satellites (e.g., Landsat-5 compared to Landsat-7)
  - Following a maneuver (e.g., star tracking)
- Needs:
  - Sub-pixel accuracy
  - Robustness to recurring use
  - Speed and High-Level of Autonomy (Near- or Near-real time applications, e.g., disaster management)
  - On-the-ground or On-Board Processing

Challenges in Image Integration and Fusion for Remote Sensing

- Same challenges than registration:
  - Various spectral and spatial resolutions
  - Acquired at different times, under different conditions
  - For example: Time series over a large number of years involving multiple programs and/or instruments
- Misregistration error
- Difficulty in quality assessment because of the lack of reference against which one may compare properties of the fused image; validation often done by the end-application not at the time of the fusion
  - Objective function often missing
  - Measures such as correlation, entropy, etc.

Challenges with Atmospheric and Cloud Interactions

Baja Peninsula, California; 4 different times of the day (GOES-8)

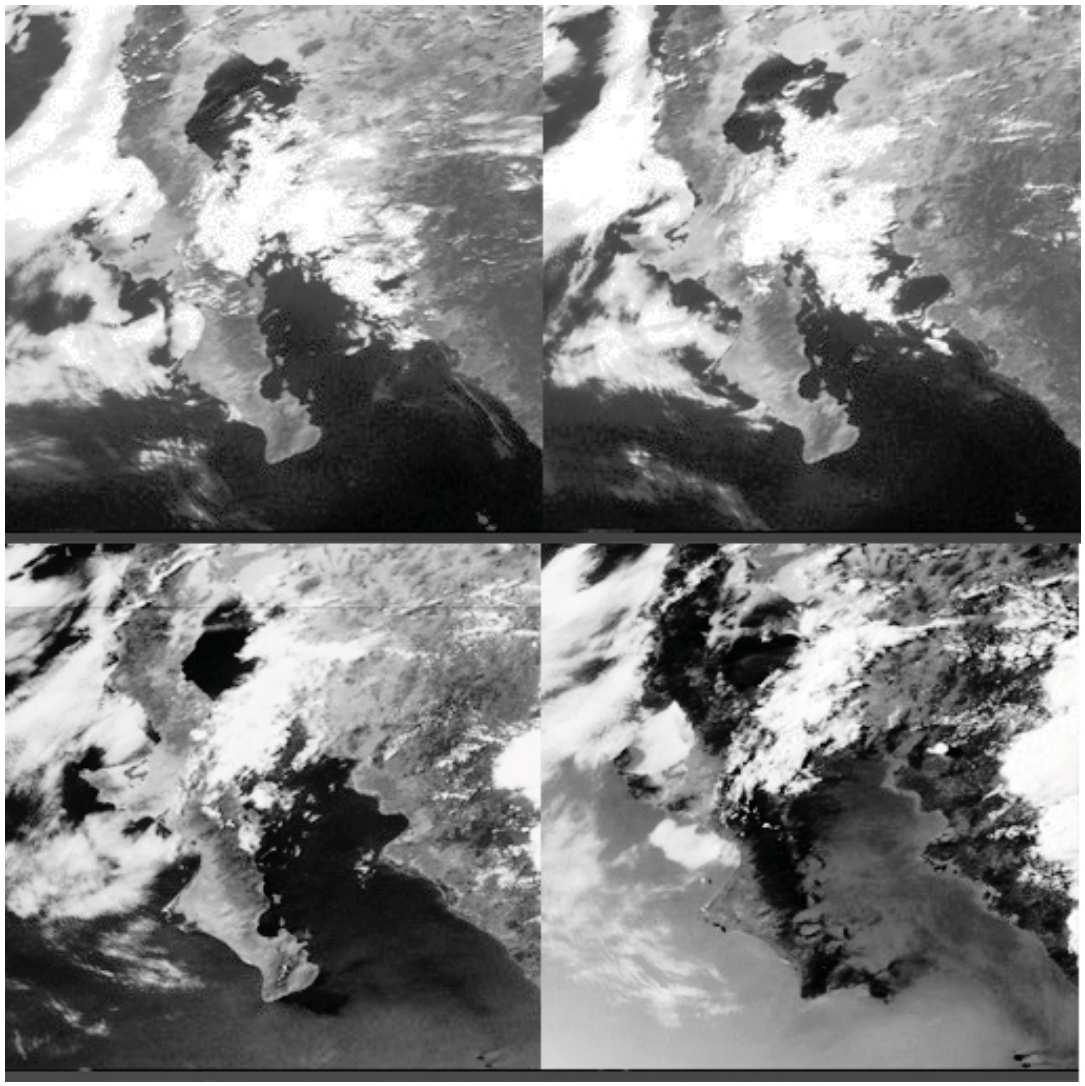

Challenges with Multitemporal Effects

Mississippi and Ohio Rivers before & after Flood of Spring 2002 (Terra/MODIS)

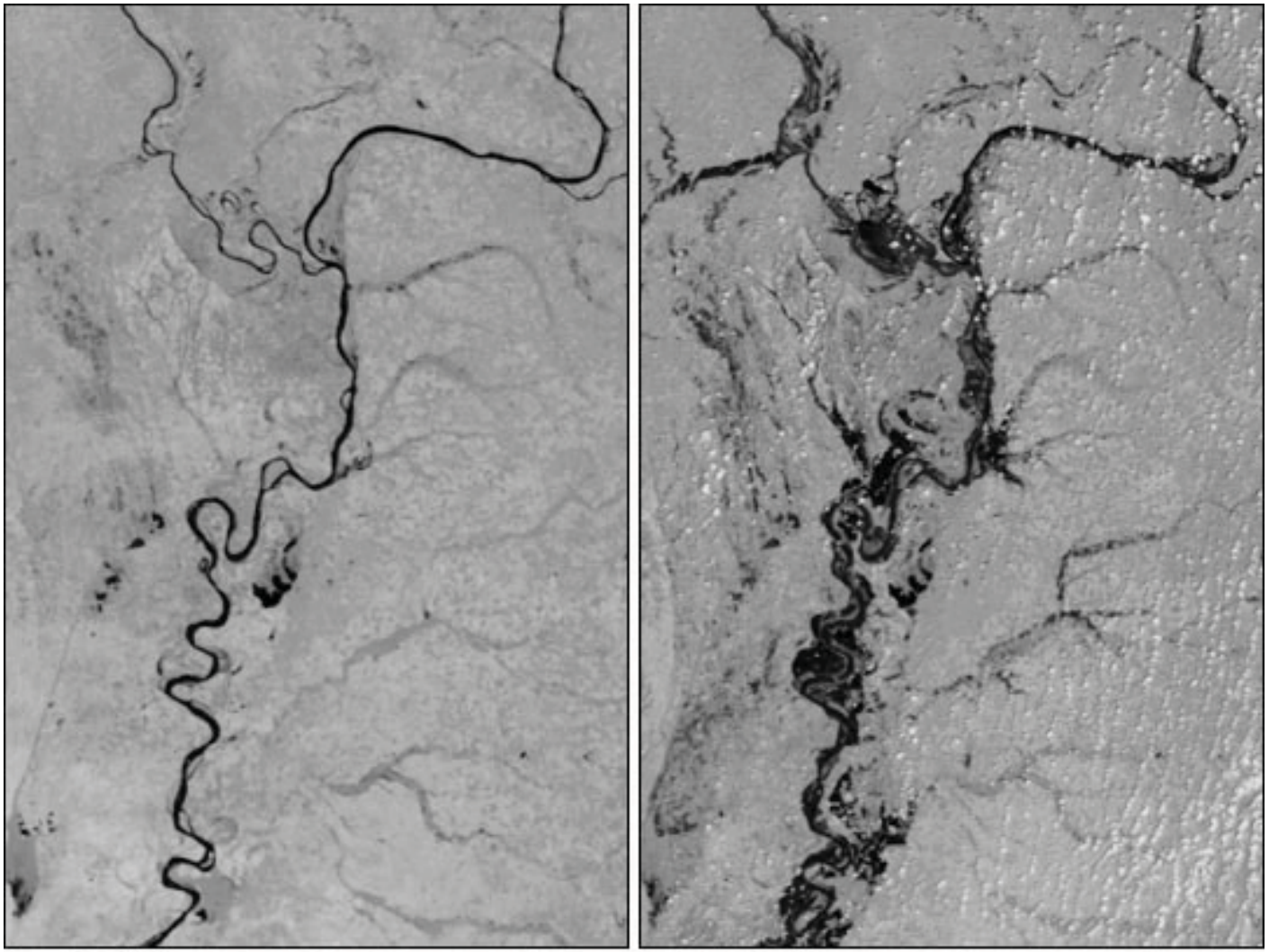

April 25, 2002

May 18, 2002

Challenges with Relief Effect

SAR and Landsat-TM Data of Lopé Area, Gabon, Africa

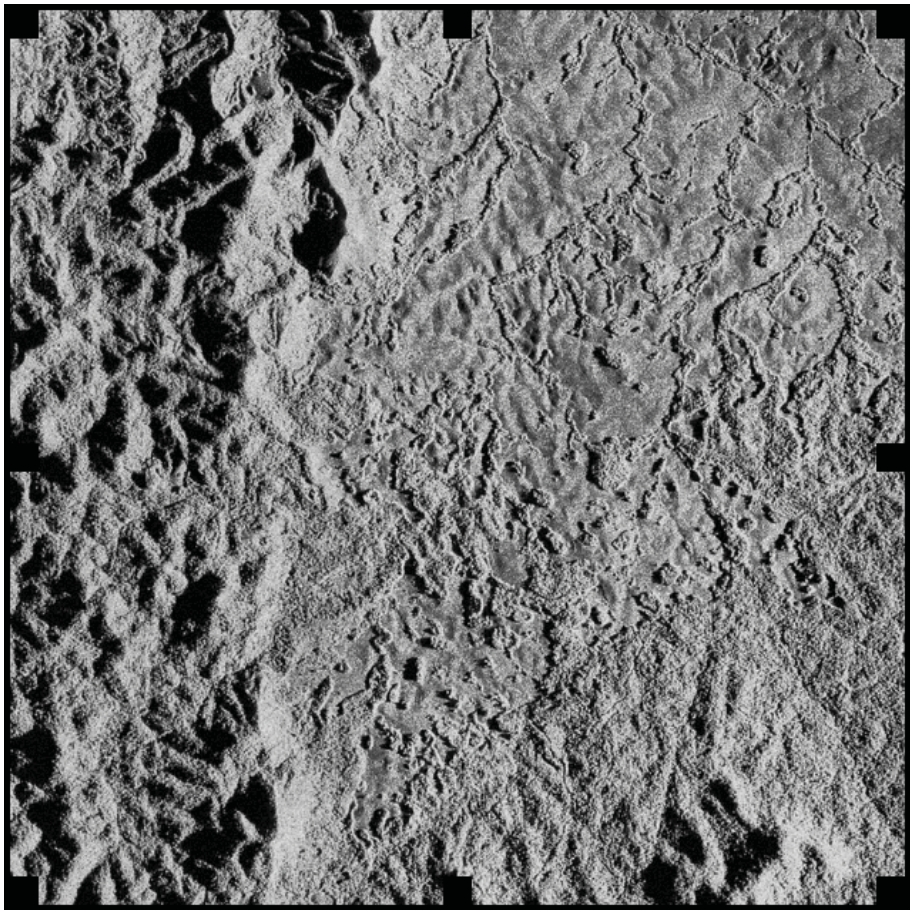

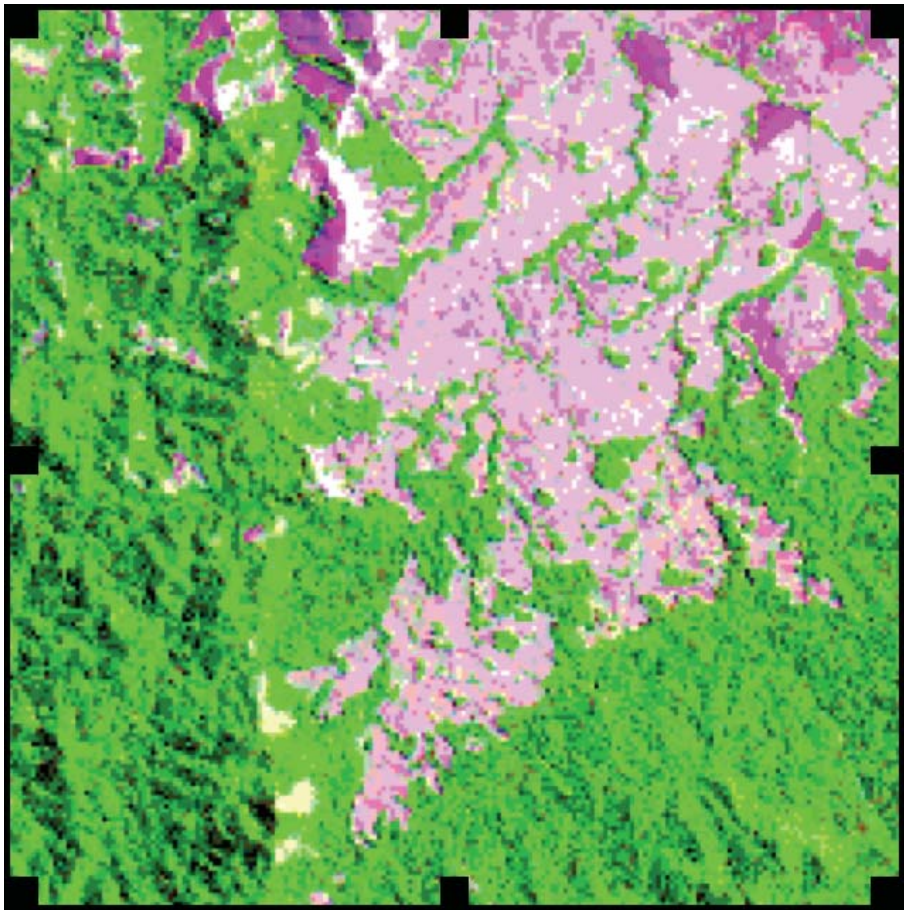

Challenges with Relief Effect (2)

Use Digital Terrain Models (DEMs) => Taking terrain into account in matching

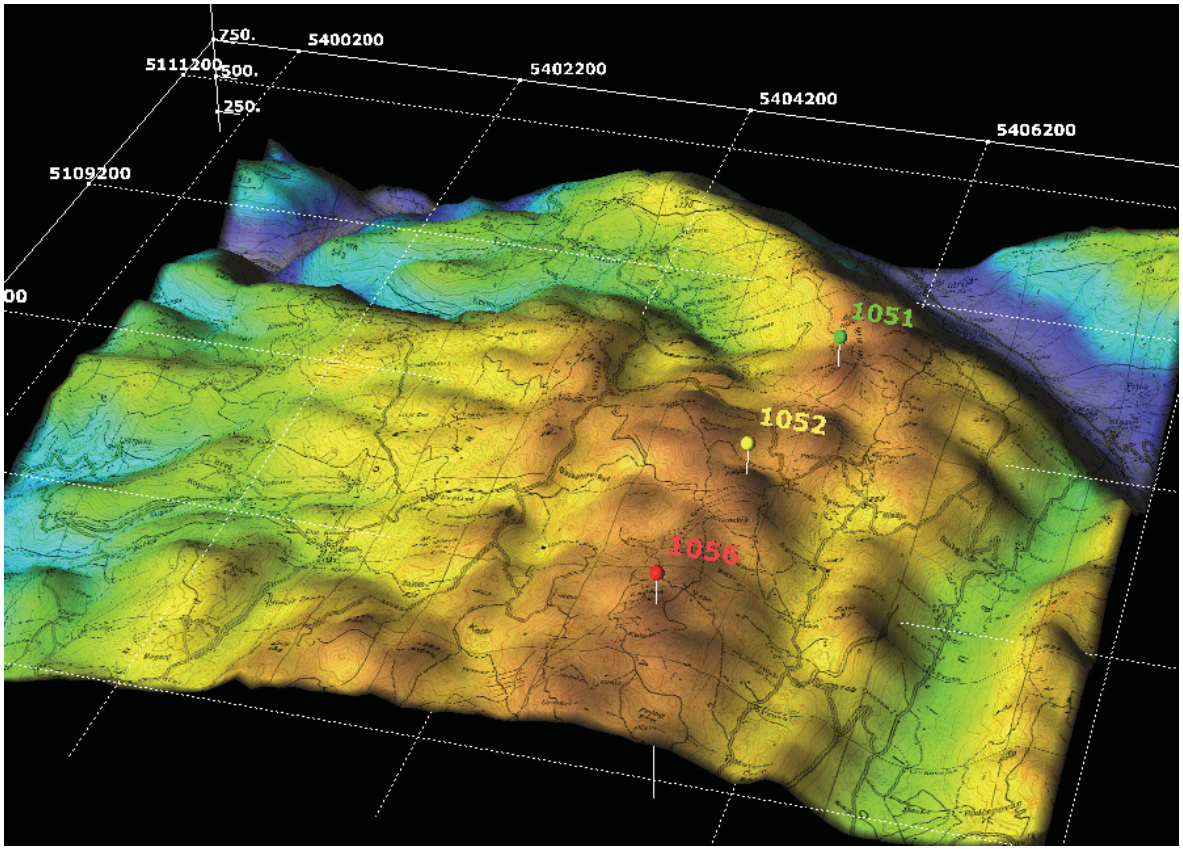

Theoretical vs. Operational Approaches for Image Registration

- Many promising theoretical approaches with good results on specific datasets, but no gold standard algorithm for operational use
- Every instrument has a working operational approach, often solved the same way (e.g., with Normalized Cross Correlation)
- Operational Team Requirements:
  - Know models of sensor/platform/etc.
  - Have access to complete data set
  - Have continuing demands/responsibility
  - Are registering same plots of land again and again – can invest effort in data preparation
  - Can't take big risks on not fully proven methods
- **Do not need one magic method – need toolbox of many approaches**

Challenges with Institutional Challenges

- Different communities/literature/requirements
  - Photogrammetry
  - Computer vision/image processing
  - Operational teams
  - Remote sensing/Earth scientists/end users
- Demanding/varying mission requirements
  - Caution in system design, new methods
- Difficulty to share data or models between instruments
- Understanding the requirements
  - Know what data is used for
  - Have to fuse many data sets
  - Have access to ancillary data
  - Know cultural and historical data

Precision Correction in Operational Systems

Some Examples - Highlights

- *AVHRR:* AUTONAV algorithm computes attitude corrections using Maximum Cross-Correlation (MCC) method between sequential images
- *GOES/METEOSAT:* CPs and NOAA Shoreline database (GSHHS) used to match edges extracted from meteorological images
- *LANDSAT:* CP image chips (1m orthorectified) using Gaussian pyramid, automatic Moravec window extraction and NCC or Mutual Information
- *MISR:* Database of 120 GCPs (each a collection of nine geolocated image patches of a well-defined and easily identifiable ground features, from Landsat, terrain-corrected, data) &ray casting simulation software
- *MODIS:* Biases and trends in the sensor orientation determined from automated control point (CP) matching and removed by updating models of the spacecraft and instrument orientation; finer CGPs from Landsat TM and ETM aggregated using PSFs and correlated with NCC
- *SEAWIFS:* Reference catalog of islands GCPs and matching using spectral classification and clustering of data, “nearest neighbor” and pattern matching techniques
- *SPOT:* Reference3D^{TM} using DEM ortho-rectified simulated reference image in focal plane geometry, matching of input image to simulated using NCC and resampling into a cartographic reference frame
- *VEGETATION:* Database of CPs from SPOT for VEGETATION1 and VEGETATION1 for VEGETATION2; Matching by NCC

Precision Correction in Operational Systems (2)

- Operational Environment
  - Platform/sensor models integrated
  - Historical data available for statistics/modeling
  - Robustness and consistency over time is a requirement
- General Characteristics
  - Use database of Ground Control Points (GCP) or Chips
  - Normalized Cross-Correlation (NCC) is the most common similarity measure
  - Digital Elevation Model (DEM) is rarely integrated in the registration process
  - Cloud masking usually integrated
  - Errors in the [0.15-0.5] range
- Various approaches. No gold standard approach:
  - Create framework to validate new image registration components and algorithms
  - For each algorithm, define “region of convergence” and “region of divergence”
  - Provide guidance/recommendations for utilization of algorithms and their components
  - Provide fast algorithms for real-time/near-real-time and on-board applications

Section 1b
Brief survey of registration, integration and fusion methods

Brief Image Registration Survey

Image Registration Frameworks

- Mathematical Framework
  - I1(x,y) and I2(x,y): images or image/map
    - find the mapping (f,g) which transforms I1 into I2:

      I2(x,y) = g(I1(fx(x,y),fy(x,y)) + n(x,y)

      - **f** : spatial mapping
      - **g**: radiometric mapping
      - **n**: sensor and other imaging noise
  - Spatial Transformations "**f**"
    - Translation, Rigid, Affine, Projective, Perspective, Polynomial, …
  - Radiometric Transformations "**g**" (Resampling)
    - Nearest Neighbor, Bilinear, Cubic Convolution, …

- Algorithmic Framework (Brown, 1992)
  1. Feature Extraction
  2. Feature Matching (Similarity Metrics & Matching Strategy)
  3. Image Resampling (if needed)

Image Registration Components

0 Pre-Processing

- Cloud Detection, Region of Interest Masking, …

1 Feature Extraction ("Control Points")

- Gray Levels, Salient Points (e.g., Edges, Edge-like such as Wavelet Coefficients, Corners), Lines, Contours, Regions, Scale Invariant Feature Transform (SIFT), etc.

2 Feature Matching

- Choice of Spatial Transformation (**function f**: a-priori knowledge)
- Choice of Search Strategy :
  - Global vs Local, Multi-Resolution, Optimization, ...
- Choice of Similarity Metrics
  - L2-Norm, Normalized Cross-Correlation, Mutual Information, Hausdorff Distance, …

3 Remapping/Resampling (**function g**: if necessary)

General Approaches to Registration

1. Manual Registration
2. Correlation-Based Methods
3. Fourier-Domain and Other-Transform Based Approaches
4. Mutual Information and Distribution-Based Approaches
5. Feature-Point Methods
6. Contour- and Region-Based Approaches

Feature Extraction

- Gray levels
- Salient points
  - Edge-like, wavelet coefficients (Simoncelli and Freeman ‘95)
  - Corners (Kearny *et al*. ‘87, Harris and Stephens ’88, Shi and Tomasi ‘94)
- Lines
- Contours, regions (Govindu *et al*. ‘99)
- Scale invariant feature transform (SIFT), Lowe ‘04

Similarity Metrics

- **L_2-norm:**
  - Minimize the sum of squared errors (SSD) over overlapping subimage

$$SSD(x,y) = \sum_{m=0}^{M-1}\sum_{n=0}^{N-1}\left[I_1(m,n) - I_2(m-x,n-y)\right]^2$$

- **Cross-correlation**
  - Maximize *cross-correlation* over image overlap

$$I_1(x,y) \circ I_2(x,y) = \sum_{m=0}^{M-1}\sum_{n=0}^{N-1} I_1(m,n) I_2(x+m,y+n)$$

- **Normalized cross-correlation (NCC)**

$$NCC_{I_1,I_2}(x,y) = \frac{\sum_{m=0}^{M-1}\sum_{n=0}^{N-1}\left[I_1(m,n) - \bar{I}_1\right]\left[I_2(x+m,y+n) - \bar{I}_2\right]}{\sqrt{\sum_{m=0}^{M-1}\sum_{n=0}^{N-1}\left[I_1(m,n) - \bar{I}_1\right]^2 \cdot \sum_{m=0}^{M-1}\sum_{n=0}^{N-1}\left[I_2(x+m,y+n) - \bar{I}_2\right]^2}}$$

Similarity Metrics (2)

- **Mutual information (MI):**

  Maximizes the degree of statistical dependence between the images

$$MI\left(I_1, I_2\right) = \sum_{g_1} \sum_{g_2} p_{I_1,I_2}\left(g_1, g_2\right) \cdot \log\left(\frac{p_{I_1,I_2}\left(g_1, g_2\right)}{p_{I_1}\left(g_1\right) \cdot p_{I_2}\left(g_2\right)} \right),$$

  or using histograms, maximizes

$$MI\left(I_1, I_2\right) = \frac{1}{M} \sum_{g_1} \sum_{g_2} h_{I_1,I_2}\left(g_1, g_2\right) \cdot \log\left(\frac{M h_{I_1,I_2}\left(g_1, g_2\right)}{h_{I_1}\left(g_1\right) \cdot h_{I_2}\left(g_2\right)} \right)$$

  where M is the sum of all histogram entries, i.e., number of pixels (in overlapping subimage)

Similarity Metrics (3)

- **Partial Hausdorff distance (PHD):**

$$H_K(I_1, I_2) = K^{th}_{p_1 \in I_1} \min_{p_2 \in I_2} \text{dist}(p_1, p_2),$$

where $1 \le K \le |I_1|$ (Huttenlocher *et al.* '93, Mount *et al.* '99)

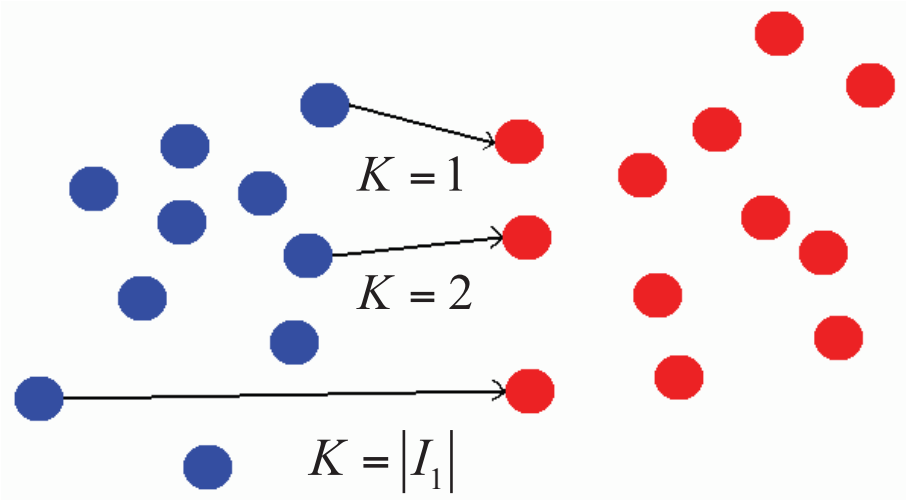

Similarity Metrics (4)

- **Discrete Gaussian mismatch (DGM):**

$$w_\sigma(a) = \exp\left(-\frac{\text{dist}(a, I_2)^2}{2\sigma^2}\right)$$

where $w_\sigma(a)$ denotes the *weight* of point *a,* and

$$\text{DGM}_\sigma(I_1, I_2) = 1 - \frac{\sum_{a \in I_1} w_\sigma(a)}{|I_1|}$$

is similarity measure ranging between 0 and 1

Transformation Functions

- Translation-only, rigid
- Rotation, scale, and translation (RST)
- Affine (6 degrees of freedom)

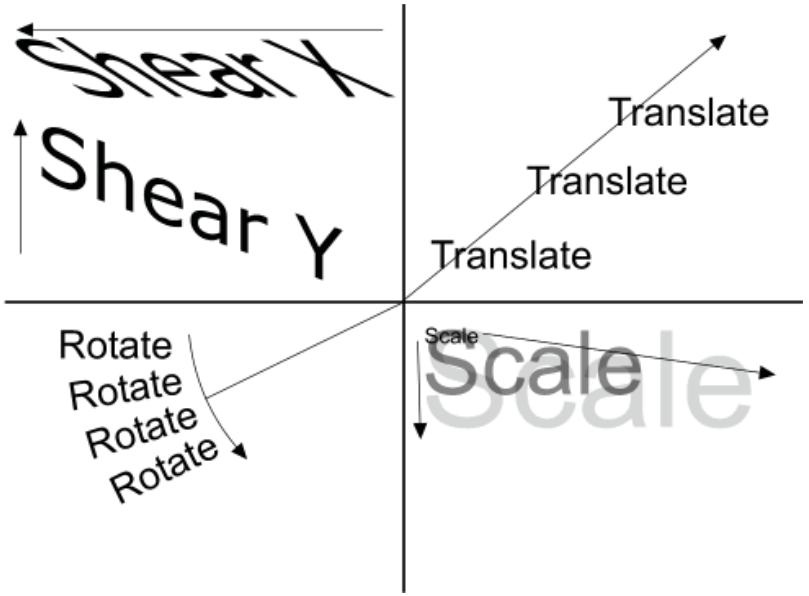

$$x' = s\cos\theta \cdot x - s\sin\theta \cdot y + t_x$$

$$y' = s\sin\theta \cdot x + s\cos\theta \cdot y + t_y$$

$$T_p = \begin{pmatrix} s\cos\theta & -s\sin\theta & t_x \\ s\sin\theta & s\cos\theta & t_y \\ 0 & 0 & 1 \end{pmatrix}$$

- Projective/homography (e.g., for perspective effects in image mosaicing); 8 parameters

Transformation Functions (2)

- Weighted linear transformation; adaptive transformation, continuous and smooth, applied to multiview images with *local geometric differences*, and maps an entire image to another
  - Interpolating surface is a weighted sum of planar patches, each of which passes through a *control point* and provides a desired gradient, i.e.,

$$f(x,y) = \frac{\sum_{i=1}^{n} R_i(x,y) L_i(x,y)}{\sum_{i=1}^{n} R_i(x,y)}$$

for monotonically decreasing weight $R_i(x,y) = \left[(x-x_i)^2 + (y-y_i)^2\right]^{-1/2}$

and $$L_i(x,y) = a_i(x-x_i) + b_i(y-y_i) + F_i$$

Matching Strategies

- Exhaustive search (exponential in dimensionality of space)
- Fast Fourier transform (FFT)
- Numerical optimization (e.g., *steepest gradient descent* wrt SSD, NCC, and MI (Thévenaz, Ruttimann, and Unser (TRU) ‘98; Spall ’92)
- Robust transformation estimate (e.g., RANSAC, LMS) if (most) correspondences are known (via SIFT-like)
- “Correspondenceless”, e.g., correlation of descriptor distribution/feature consensus (Govindu *et al*. ‘99)
- Robust feature matching (RFM), e.g., efficient subdivision and pruning of transformation space; Huttenlocher *et al*. ‘93, Mount *et al*. ’99, Netanyahu *et al*. ‘04

Matching Strategies (2)

- **Frequency domain-based approach**
  - Efficient computation of correlation as inverse of $F_1^*(u,v)F_2(u,v)$
  - Practical implementation (extension to NCC, masking invalid pixels, optimized computation)
  - Finding (small) rotational and scale differences (by matching chips)
  - Subpixel registration for translation-only using *phase* estimate (also in case of image aliasing)
  - Rotation and scale estimate by casting to *log-polar* coordinates

Matching Strategies (3)

- **Matched filtering**
  - Maximize SNR (using theory of linear systems)
  - Apply *phase-only* and *symmetric phase-only* matched filters for translation-only IR

$$\text{Phase product} = \frac{F_1^*(u,v)}{\left|F_1(u,v)\right|}\frac{F_2(u,v)}{\left|F_2(u,v)\right|} = e^{-j(ut_x+vt_y)}$$

  - Apply *Fourier-Mellin transform* for rotation and scale changes; transform represents these parameters as translational shifts in log-polar coordinates of magnitude of Fourier spectrum, i.e., first estimate rotation and scale, followed by translation estimate

Matching Strategies (4)

- **Numerical optimization**
  - Powel's, Brent's (1-D), simplex, etc.
  - **Steepest descent/ascent variants**
    - Standard $\mathbf{p}_{k+1} = \mathbf{p}_k - \lambda_k \mathbf{g}_k$
    - Newton-Raphson $\mathbf{p}_{k+1} = \mathbf{p}_k - \lambda_k \mathbf{H}_k^{-1} \mathbf{g}_k$
    - Levenberg-Marquardt $\mathbf{p}_{k+1} = \mathbf{p}_k - \left(\mathbf{H}_k + \lambda_k \mathrm{diag}\left[\mathbf{H}_k\right]\right)^{-1} \mathbf{g}_k$
      - Apply to various similarity metrics, e.g., SSD (Eastman and Le Moigne '01), Mutual Information, etc.
        - » Explicit computation of gradient (and Jacobian/Hessian), e.g., Thévenaz and Unser '00
        - » Stochastic approx. (Spall '92; Cole-Rhodes *et al.* '03)

Matching Strategies (5)

- **Alignment via local geometric distributions**

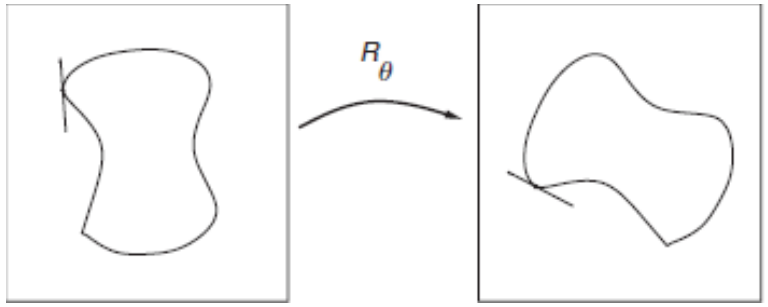

Rotated contours

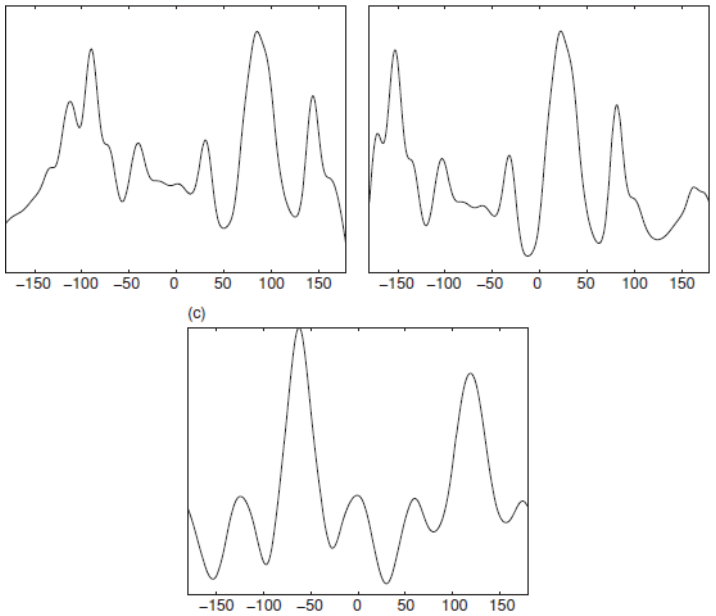

Slope angle distributions and their correlation

Matching Strategies (6)

- **Robust feature matching (RFM)**
  - **Space of affine transformations**: 6-D space
  - ***Subdivide***: Quadtree or kd-tree. Each cell T represents a set of transformations; T is *active* if it may contain t_{opt}; o/w, it is *killed*
  - ***Uncertainty regions* (UR's)**: Rectangular approximation to the possible images $\tau(a)$ for all $\tau \in T, a \in I_1$
  - ***Bounds***: Compute *upper bound* (on optimum similarity) by sampling a transformation and *lower bound* by computing *nearest neighbors* to each UR
  - ***Prune***: If lower bound exceeds best upper bound, then kill the cell; o/w, split it

Matching Strategies (7)

- **Computational efficiency**
  - "Culling" feature points via, e.g., *condition theory*
  - Efficient numerical or discrete algorithmic procedures
  - Hierarchical pyramid-like (wavelet) decomposition
  - Use landmark chip database (instead of a large scene) or alternatively, extract automatically corresponding regions of interest using *mathematical morphology* (Plaza *et al* '07)

Brief Image Fusion Survey

Methods of Image Fusion

- **Prerequisite to Image Fusion:** Very accurate registration
- **Various Approaches** [Blum and Liu, 2005]**:**
  - Multiscale-Decomposition-Based Fusion Methods

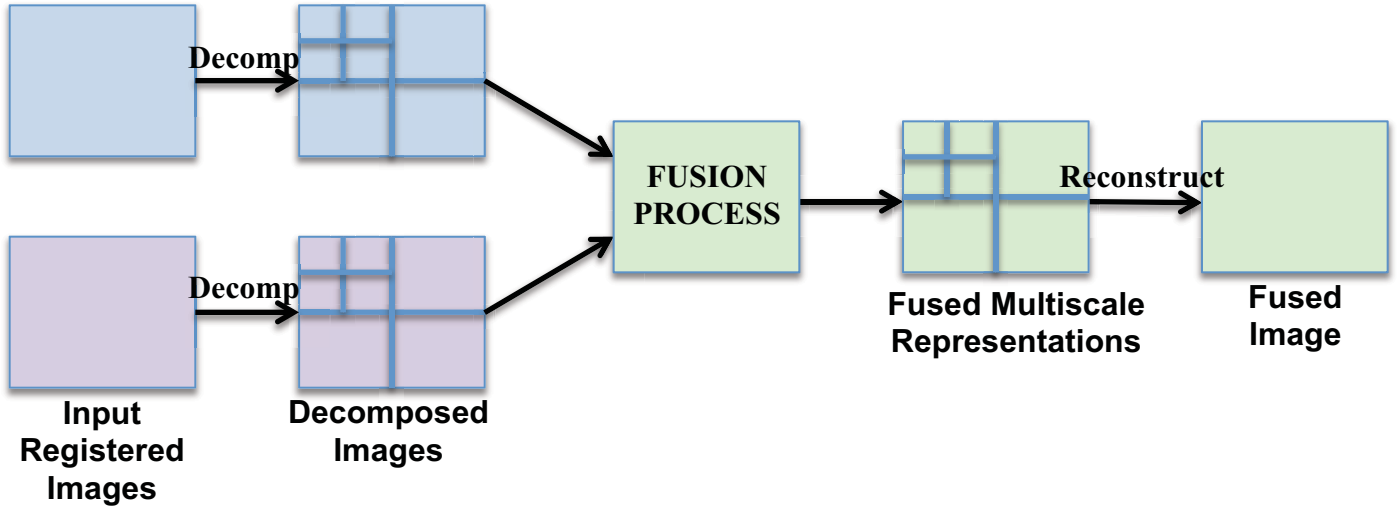

1. Multiscale representations: Pyramid Transform (e.g., Laplacian), Discrete Wavelet Transform (DWT) and Discrete Wavelet Frame (DWF)
2. Activity-level measurement
3. Coefficient Grouping Method
4. Coefficient Combining Method
5. Consistency Verification

Methods of Image Fusion (2)

- NonMultiscale-Decomposition-Based Methods
  - Pixel-Level Weighted Averaging
    - e.g., PCA
  - Non-Linear Method
    - e.g., separate images into low-pass (LP) and high-pass (HP); then modify and fuse LP and HP
  - Estimation Theory Based Methods
    - e.g. using Maximum A Priori (MAP) and Maximum Likelihood (ML) estimates or Markov Random Field (MRF) distributions
  - Color Composite Fusion
    - Combines input images in color space => false color representation
    - Often used with another method, e.g., PCA or Neural Network
  - Artificial Neural Networks
    - e.g., trained to superimpose objects of interest on background

Performance Evaluation of Fusion Algorithms

- Objective Evaluation using a Reference Image
  - Root Mean Square Error (*RMSE*)

$$RMSE = \sqrt{\left(\frac{1}{NM} \sum_{i=1}^{N} \sum_{j=1}^{M} \left| R(i,j) - F(i,j) \right|^2 \right)}$$

    - » Where R is the reference image, F the fused image, and NxM the size of the image
  - Correlation
  - Peak Signal to Noise Ratio (*PSNR*)

$$PSNR = 10 \log_{10} \left(\frac{L^2}{\frac{1}{NM} \sum_{i=1}^{N} \sum_{j=1}^{M} \left| R(i,j) - F(i,j) \right|^2} \right)$$

    - » Where L is the number of gray levels in the image

Performance Evaluation of Fusion Algorithms (2)

- Objective Evaluation using a Reference Image (cont.)
  - Mutual Information (MI)
  - Universal Quality Index (QI) (Wang and Bovik, 2002)

$$Q = \frac{4\sigma_{xy}\bar{x}\bar{y}}{(\sigma_x^2 + \sigma_y^2)[(\bar{x})^2 + (\bar{y})^2]}$$

    - » Where $\bar{x}$ *and* $\bar{y}$ represent the average of all pixels in the reference and the fused images, respectively,
    - » σ_x^2 *and* σ_y^2 represent the respective variances and σ_{xy} represents the co-variance between the 2 images
  - – Other indexes derived from QI, (e.g., (Piella et al, 2003) where index based on the local saliencies of the input images)

Performance Evaluation of Fusion Algorithms (3)

- Objective Evaluation without a Reference Image
  - Standard Deviation (SD)
  - Entropy (H)
  - Overall Cross Entropy of the source images X, Y and the fused image F

$$CE(X,Y;F) = \frac{CE(X;F)+CE(Y;F)}{2}$$

with

$$CE(X;F) = \sum_{i=0}^{L} h_x(i) \log_2 \left(\frac{h_X(i)}{h_F(i)} \right)$$

» Where h is the normalized histogram of the image

References …

- L. Wald, “Some terms of reference in data fusion,” IEEE Transactions on Geoscience and Remote Sensing, Vol. 37, No. 3, 1999, pp. 1190-1193. Also at http://www.data-fusion.org/terms_of_reference
- J.R. Townshend, C.O. Justice, C. Gurney, and J. McManus, “The impact of misregistration on change detection,” IEEE Transactions on Geoscience and Remote Sensing, Vol. 30, No. 5, 1992, pp. 1054-1060.
- X. Dai and S. Khorram, “The effects of image misregistration on the accuracy of remotely sensed change detection,” IEEE Transactions on Geoscience and Remote Sensing, Vol. 36, No. 5, 1998, pp. 1566-1577.
- L.G. Brown, “A survey of image registration techniques,” ACM Computing Surveys, Vol. 24, No. 4, 1992, pp. 325-376.
- J. Le Moigne, N.S. Netanyahu, and R.D. Eastman, Image Registration for Remote Sensing, Cambridge University Press, 2011.
- E.P. Simoncelli and W.T. Freeman. “*The Steerable Pyramid: A Flexible Architecture for Multi-Scale Derivative Computation,”* IEEE Second Int'l Conf on Image Processing, October 1995.
- J.K. Kearney, W.B. Thompson and D.L. Boley, “Optical flow estimation: An error analysis of gradient-based methods with local optimazation,” IEEE Transactions on Pattern Analysis and Machine Intelligence, Vol. 9 , 1987, pp. 229–244.
- C. Harris and M. Stephens, “A combined corner and edge detector,” Proceedings of the 4th Alvey Vision Conference, 1988, pp. 147-151.
- J. Shi and C. Tomasi, “Good features to track,” 9th IEEE Conference on Computer Vision and Pattern Recognition, Springer.
- V. Govindu and C. Shekhar. Alignment Using Distributions of Local Geometric Properties, IEEE Transactions on Pattern Analysis and Machine Intelligence, PAMI, October 1999.
- D.G. Lowe, “Distinctive Image Featyres from Scale-Invariant Keypoints,” International Journal of Computer Vision, Vol. 60, No. 2, 2004, pp. 91-110.

References …

- D.P. Huttenlocher, G.A. Klanderman and W.J. Rucklidge, “Comparing images using the Hausdorff distance,” IEEE Transactions on Pattern Analysis and Machine Intelligence, Vol. 15 , 1993, pp. 850–863.
- D.M. Mount, N.S. Netanyahu, and J. Le Moigne, “Efficient algorithms for robust point pattern matching’, Pattern Recognition, Vol. 32 , 1999, pp. 17–38.
- N.S. Netanyahu, J. Le Moigne and J.G. Masek, “Georegistration of Landsat data via robust matching of multiresolution features,” IEEE Transactions on Geoscience and Remote Sensing, Vol. 42 , 2004, pp. 1586-1600.
- P. Thevenaz, U. Ruttimann and M. Unser, “A pyramid approach to subpixel registration based on intensity,” IEEE Transactions on Image Processing, Vol. 7, No. 1, 1998, 27-41.
- J.C. Spall, “Multivariate stochastic approximation using a simultaneous perturbation gradient approximation,” IEEE Transactions on Automatic Control, Vol. 37, No. 3, 1992, pp. 332-341.
- A. Cole-Rhodes, K. Johnson, J. Le Moigne, and I. Zavorin, “Multiresolution registration of remote sensing imagery by optimization of mutual information using a stochastic gradient,” IEEE Transactions on Image Processing, Vol. 12, No. 12, 2003, pp. 1495-1511.
- A. Plaza, J. Le Moigne, and N.S. Netanyahu, “Parallel Morphological Feature Extraction for Automatic Registration of Remotely Sensed Images,” 2007 IEEE International Geoscience and Remote Sensing Symposium, IGARSS'07, Madrid, Spain, July 2007.
- R.S. Blum and Z. Liu (eds), “Multi-Sensor Image Fusion and its Applications,” Taylor & Francis, 2005.
- Z. Wang and A.C. Bovik, “A Universal Image Quality Index,” IEEE Signal Processing Letters, Vol. 9, No. 3, 2002, pp. 81-84.
- G. Piella and H. Heijmans, “A New Quality Metric for Image Fusion,” Proc. International Conference on Image Processing (ICIP), Sept 2003, Vol.2, pp. III-173-176.

Section 2c
Wavelets and Redundant Representations for Image Registration

Why Wavelets and Redundant Representations for Image Registration

- Representations such as the multiresolution wavelets utilized for the new compression standard JPEG-2000 can bring multisensor/multiresolution data to the same spatial resolution without losing significant information and without blurring the higher resolution data.
- At the lower resolutions, the process preserves important global features such as rivers, lakes and mountain ridges as well as roads and other man-made structures, while at the same time eliminating weak higher resolution features often considered as "noise or "spurious pixels." Of course, some of the important finer features will be lost at the lowest resolutions but, if needed, they can be retrieved in the iterative higher levels of decomposition.
- The multiresolution iterative search focuses progressively toward the final transformation with a decreasing search interval and an increasing accuracy at each iteration. Hence, this type of strategy achieves higher accuracies with higher speeds than a full search at the full resolution.
- Wavelet decomposition and multiresolution iterative search are very well-suited for fine-grained parallelization, thus speeding up the computations even more.

Wavelets for Image Registration

- 1994: First results on the utilization of orthogonal Daubechies wavelets for image registration

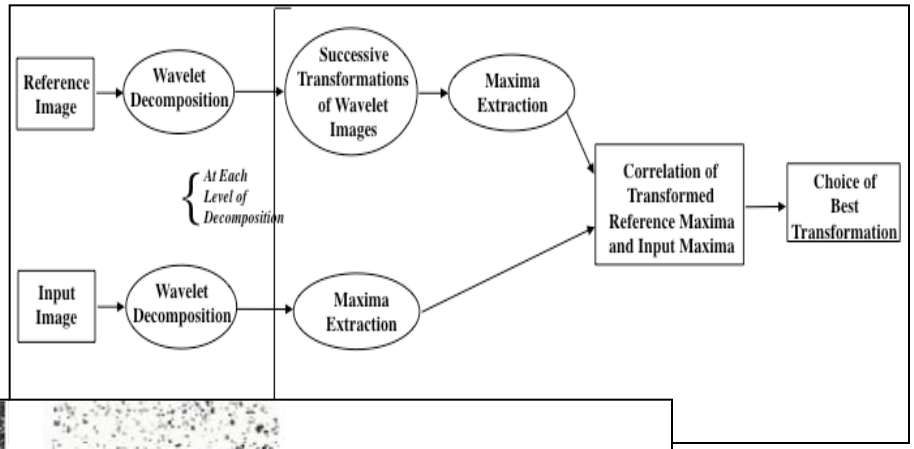

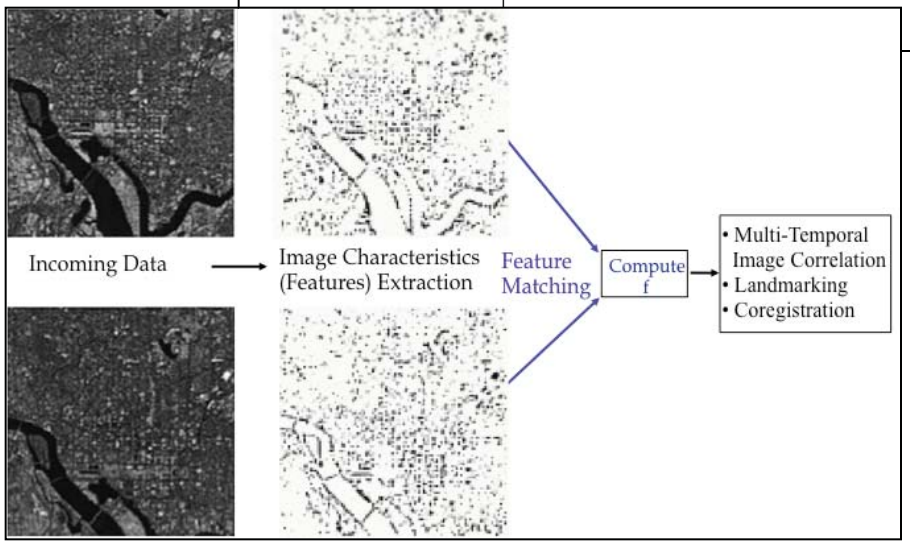

Figure 1
Original Image

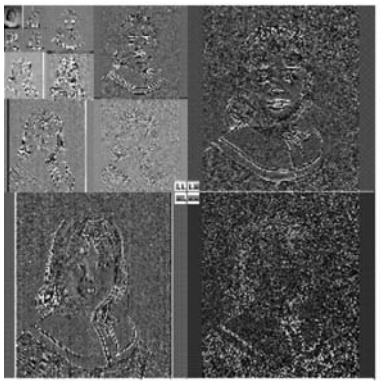

Figure 2
Wavelet Coefficients Corresponding to Figure 1

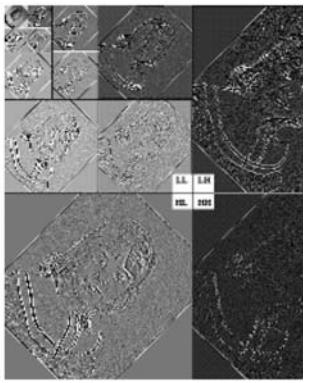

Figure 3
Wavelet Coefficients Correspond to Figure 1 rotated 44 degrees

Rotation and Translation Invariance Issues

- Orthogonal wavelets, feature information changes within or across subbands with subsampling => Study for Shift Sensitivity:
  - low-pass subband relatively insensitive to translation, if features are twice the size of wavelet filters
  - high-pass subband more sensitive but can still be used.

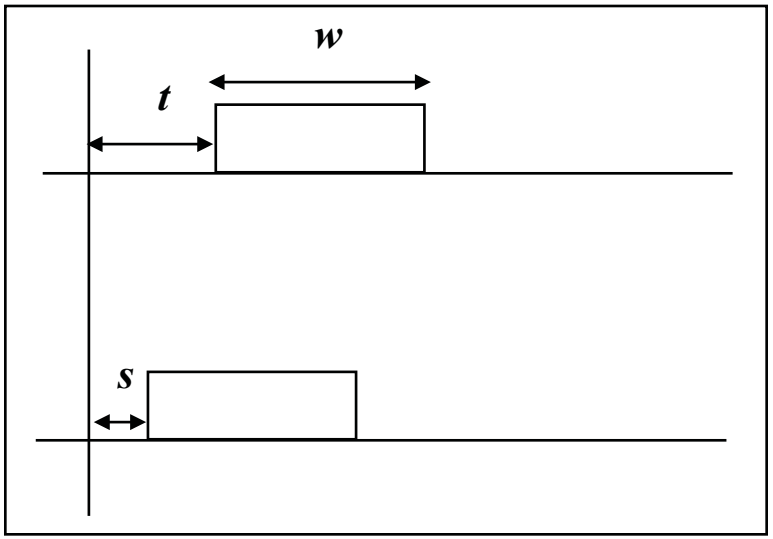

Correlate Wavelets of Two Pulses

Translation Sensitivity – Low-Pass Level 3

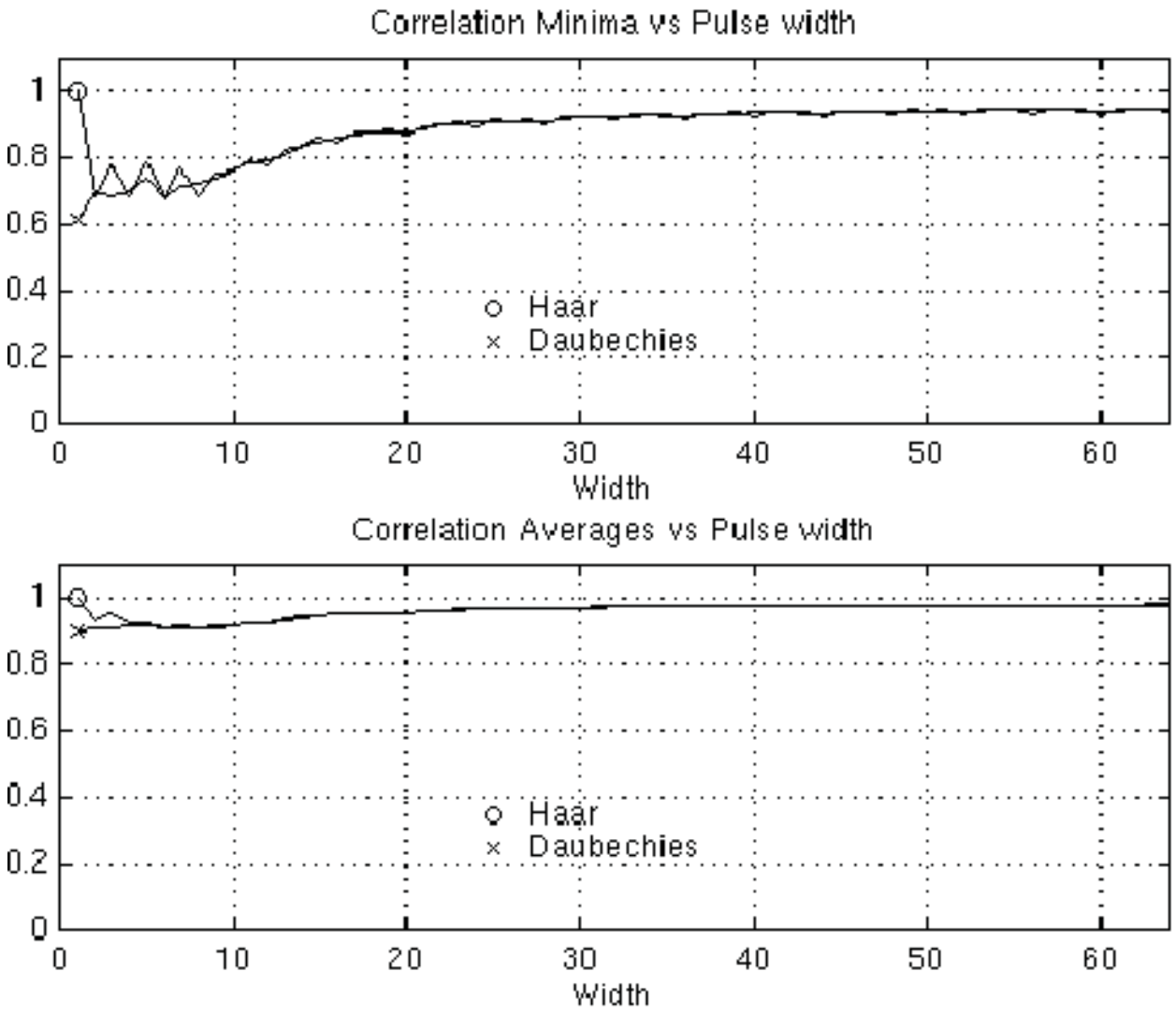

Translation Sensitivity – High-Pass Level 3

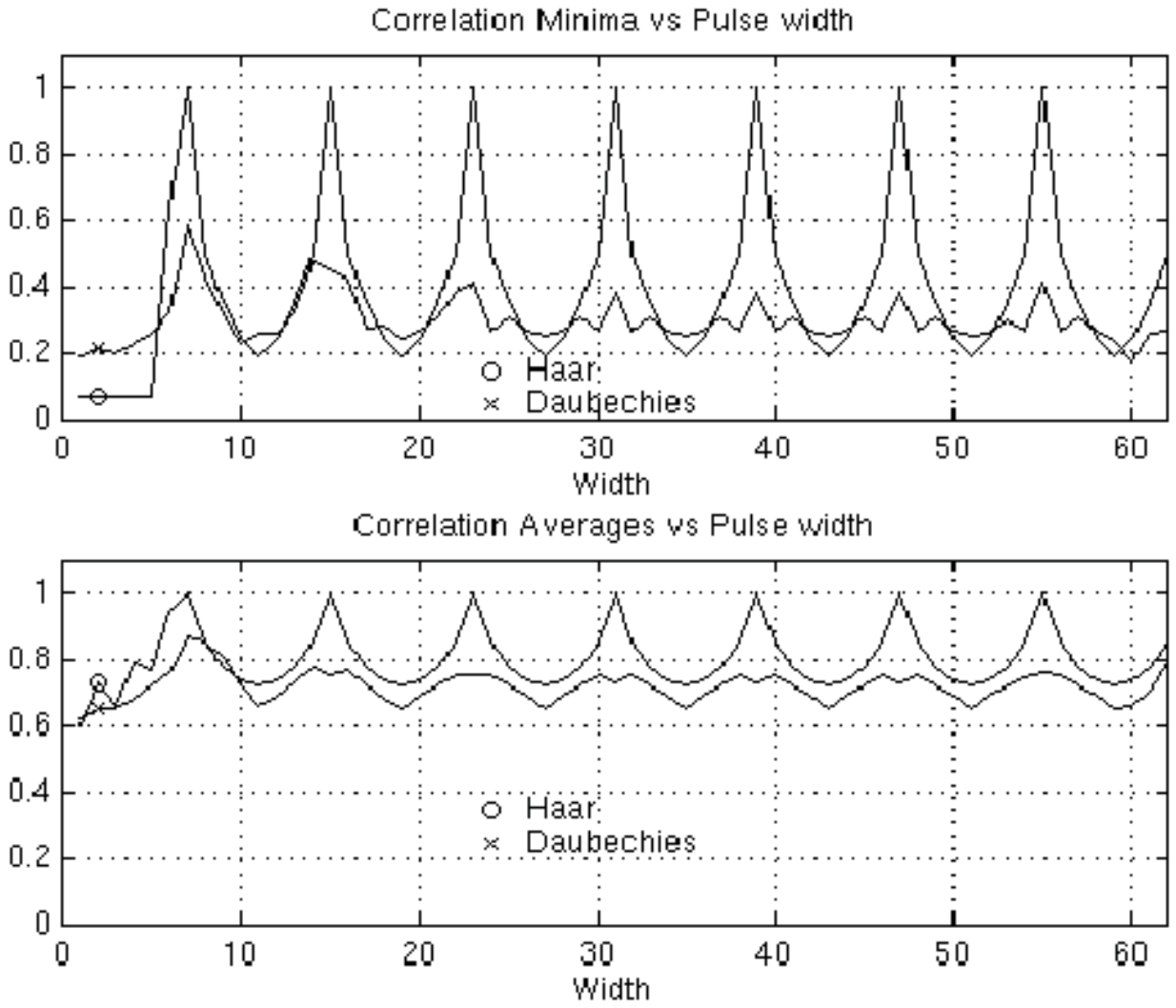

Rotation- and Translation-Invariant Representations

- Spline Wavelets [Battle & Lemarié; Unser et al]

$$V_i^n = \{g_i^n(x) = \sum_{k=-\infty}^{+\infty} c_i(k)\varphi^n(2^{-i}x-k), x \in \Re, c_i \in l_2\}$$ with scaling function $$\varphi^n(x) = \sum_{k=-\infty}^{+\infty} p(k)\beta^n(x-k)$$

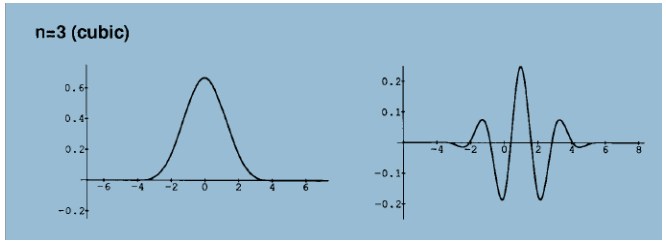

Example of B-Spline Scaling Function and Associated Wavelet

p arbitrary invertible convolution operator or filter, and $\beta^n(x)$ is a B-spline of order n (can be constructed by repeated convolution of B-Spline of order 0)

- Simoncelli et al
  - Relax critical sampling condition of wavelet transforms
  - Provides an overcomplete representation by 4k/3

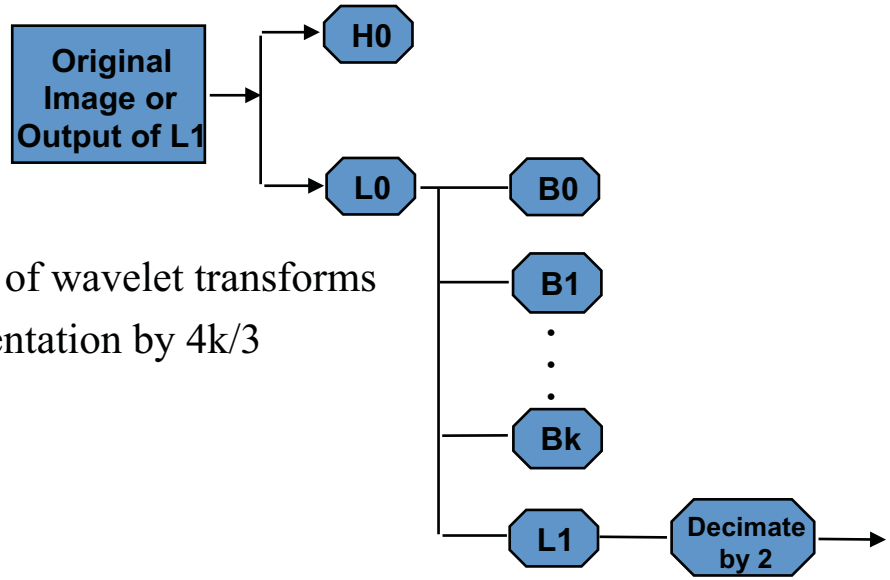

Framework for Evaluation of Image Registration Components

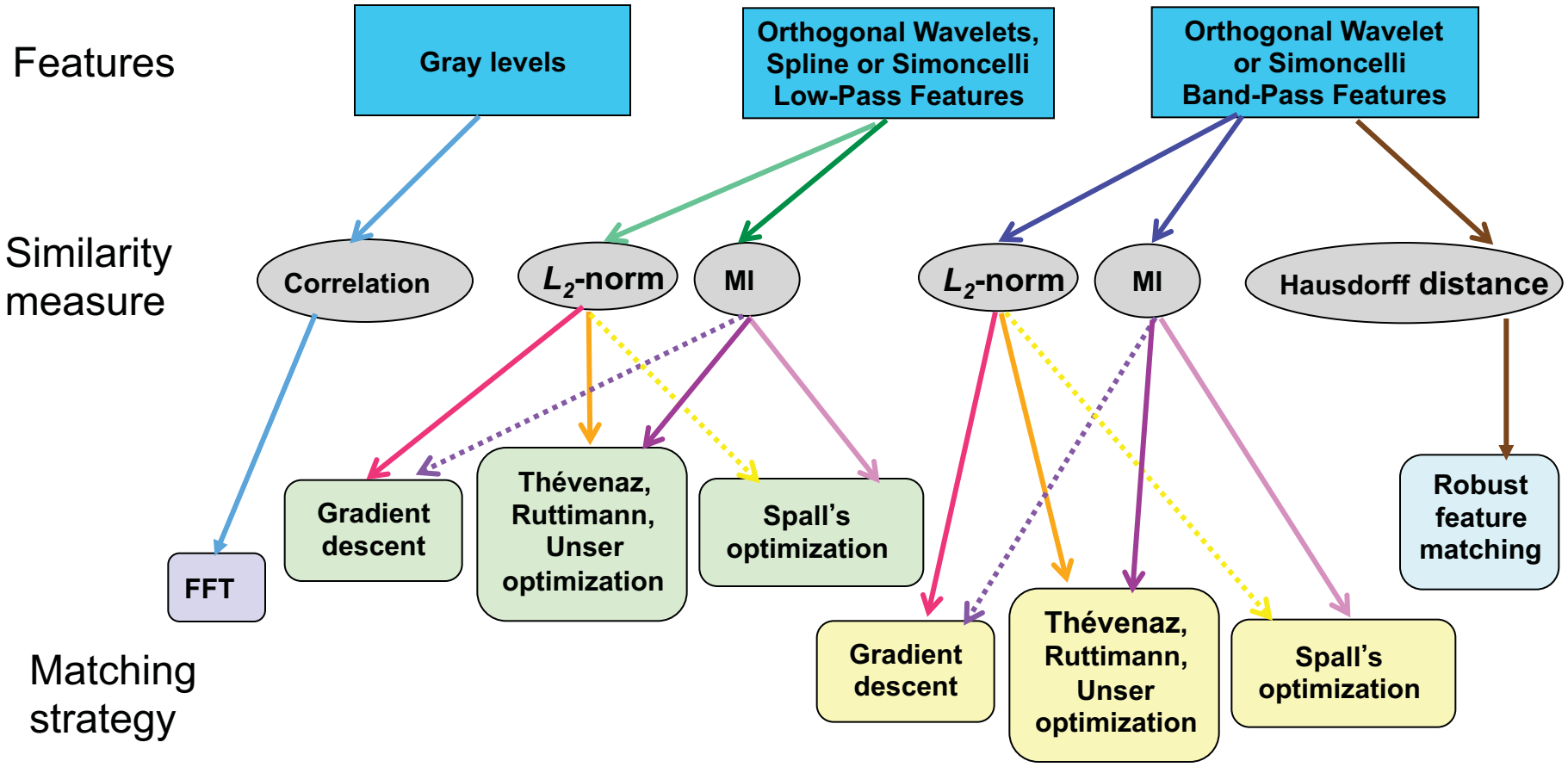

Framework for Evaluation of Image Registration Components

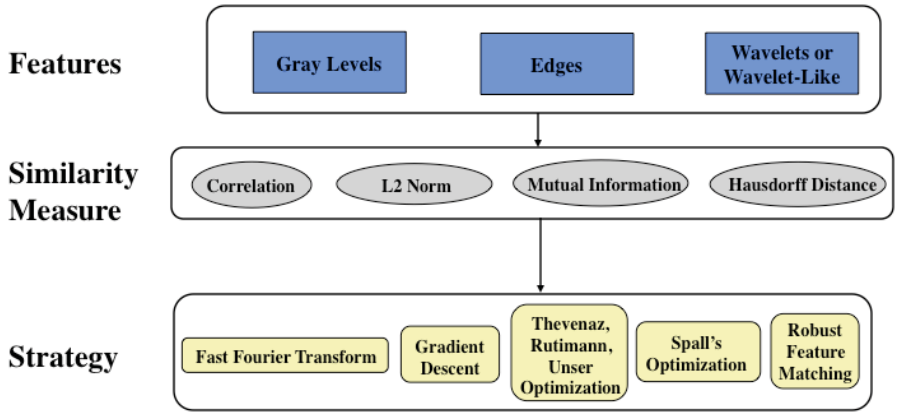

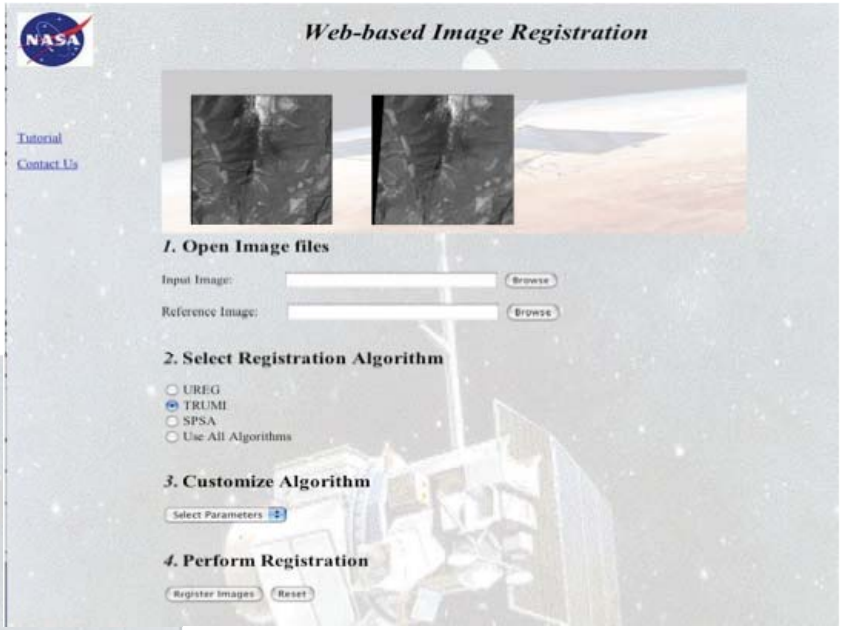

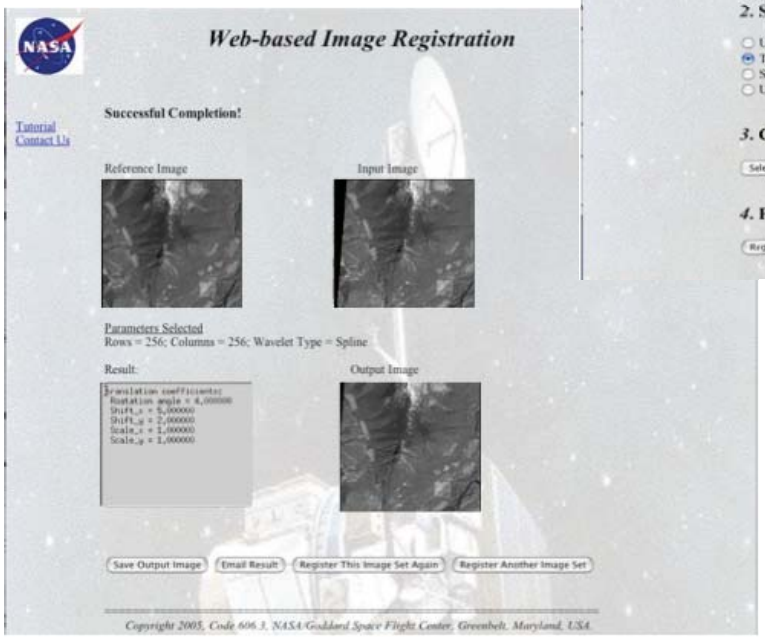

TARA (Toolbox for Automated Registration and Analysis)

Algorithm Testing Using … Synthetic Data

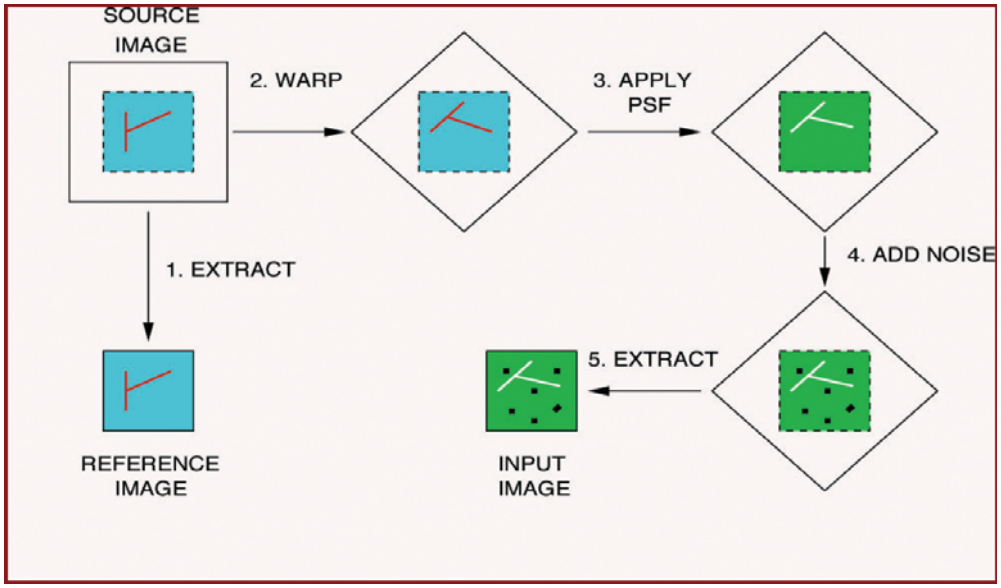

Synthetic Image Generation

Transformation of Starting Scene:

- Scales in [0.8,1.2] (step = 0.05)
- Translations in [0,20] pixels (step = 0.5)
- Rotations in [0,20] degrees (step = 0.5)
- Gaussian noise in [-15, 20] dB (step = 1)
- Radiometric Transformation (PSF constructed from black 512x512 image with 5x5 white center)

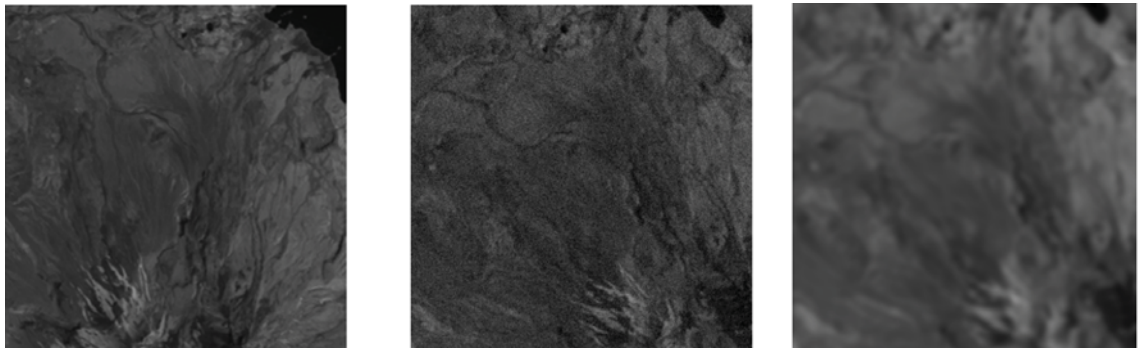

Synthetic Image Examples (Original; Warp & Noise; Warp & PSF)

Results Marquart Levenberg Optimization + L2 Similarity
Spline Wavelets and Simoncelli Features
Varying Noise – With or Without PSF [Zavorin et Le Moigne, 2005]

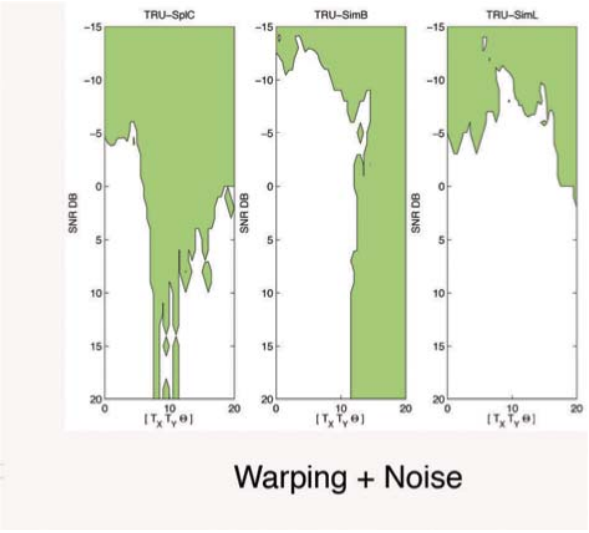

Warping + Noise

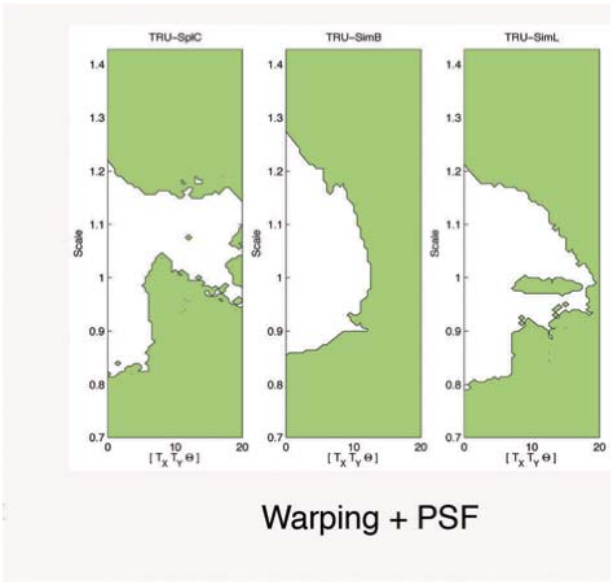

Warping + PSF

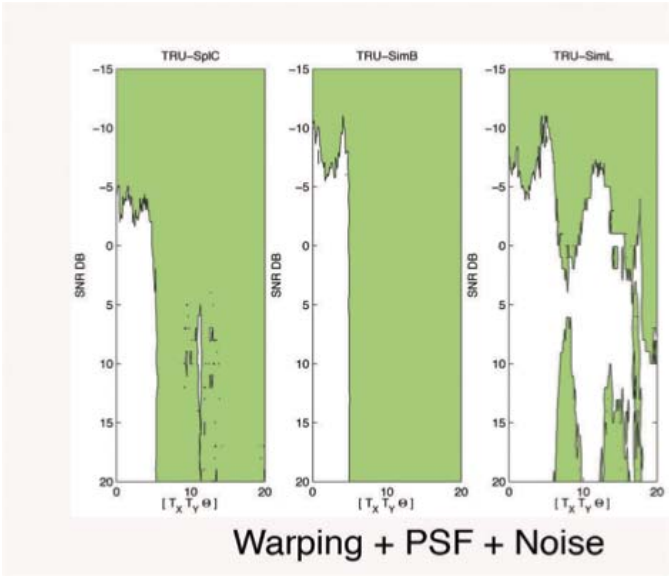

Warping + PSF + Noise

The shaded green regions in each plot correspond to those points in the parameter space for which the resulting global RMS registration error is larger than 1.0

Sensitivity to Initial Guess [Le Moigne et al, 2004]

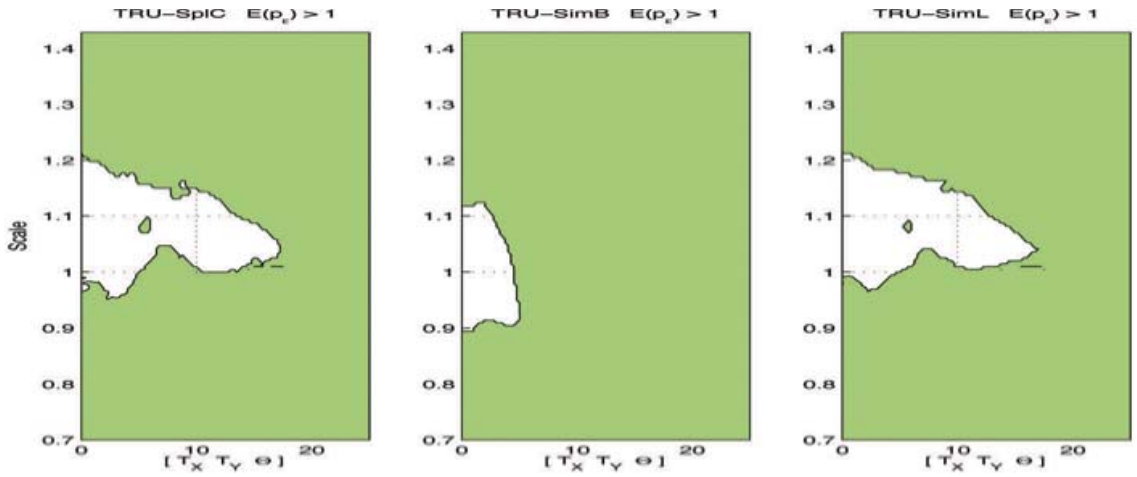

Sensitivity of TRU Algorithms to Initial Guess
(with PSF)

Overall Main Findings

- *Simoncelli-based methods outperform Spline pyramid-based methods*
- *Optimization based on Mutual Information does not perform better than L2-Norm*
- *Simoncelli/Low-Pass better than Simoncelli/ Band-Pass for Low Noise and Same Radiometry and for Initial Guess Sensitivity*

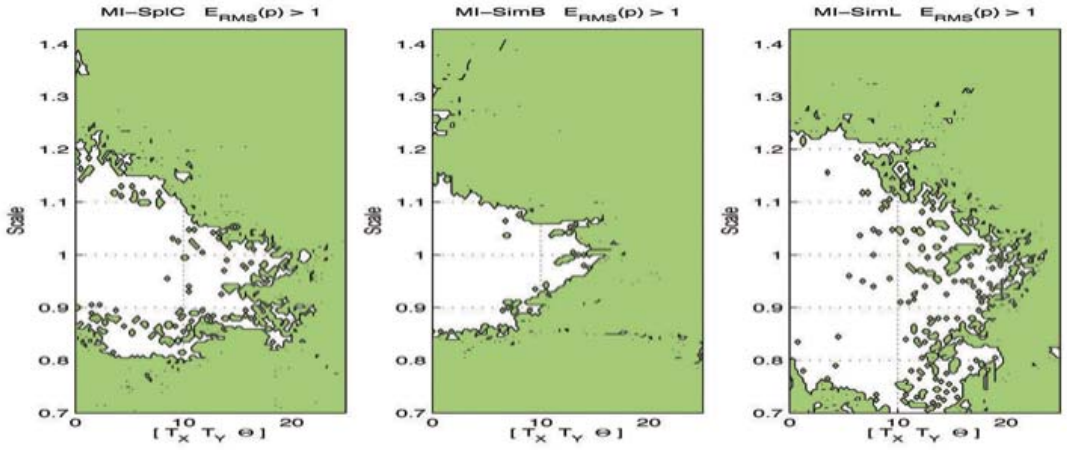

Sensitivity of TRU/MI to Initial Guess

Registration using a Chip Database

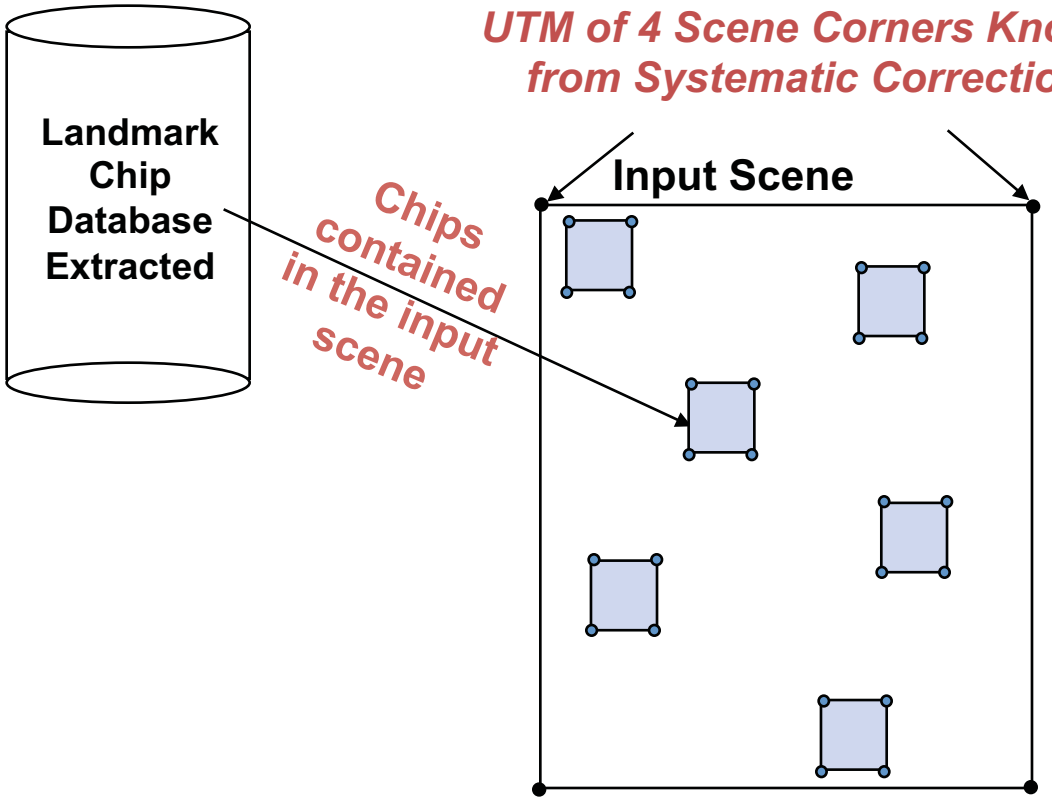

1. ***Find Chips that correspond*** **to the Incoming Scene**
2. ***For Each Chip, Extract Window*** **from input scene using UTM coordinates**
3. ***Eliminate Windows*** **with insufficient information**
4. ***Smooth and Normalize*** **gray values of both Chip and Window using a Median Filter**
5. ***Register each (Chip,Window) Pair*** **using a wavelet-based automatic registration: get a local transformation for each pair**
6. ***Eliminate Outliers***
7. ***Compute Global Rigid Transformation*** **from all local ones**
8. ***Compute Correct UTM*** **of 4 Scene Corners of input scene**
9. ***If desired, Resample*** **the input scene according to the global transformation**

Algorithm Testing Using …
Landsat-TM Multitemporal Data [Netanyahu et al, 2004]

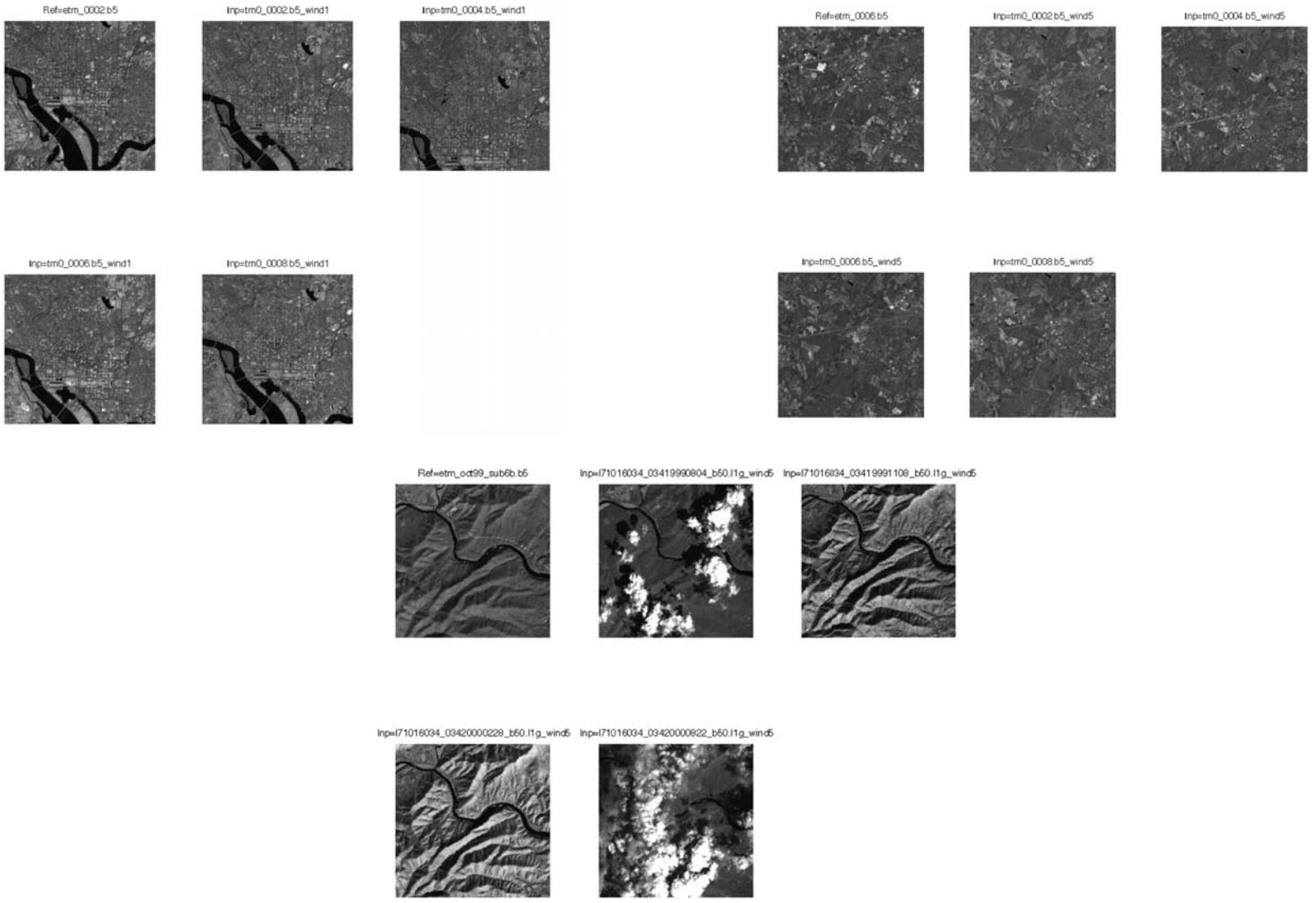

Algorithm Testing Using …
Landsat-TM Multitemporal Data (2)

- Landsat-5 and -7 Multi-Temporal Data [Netanyahu et al, 2004]:
  - Chips and Corresponding Windows

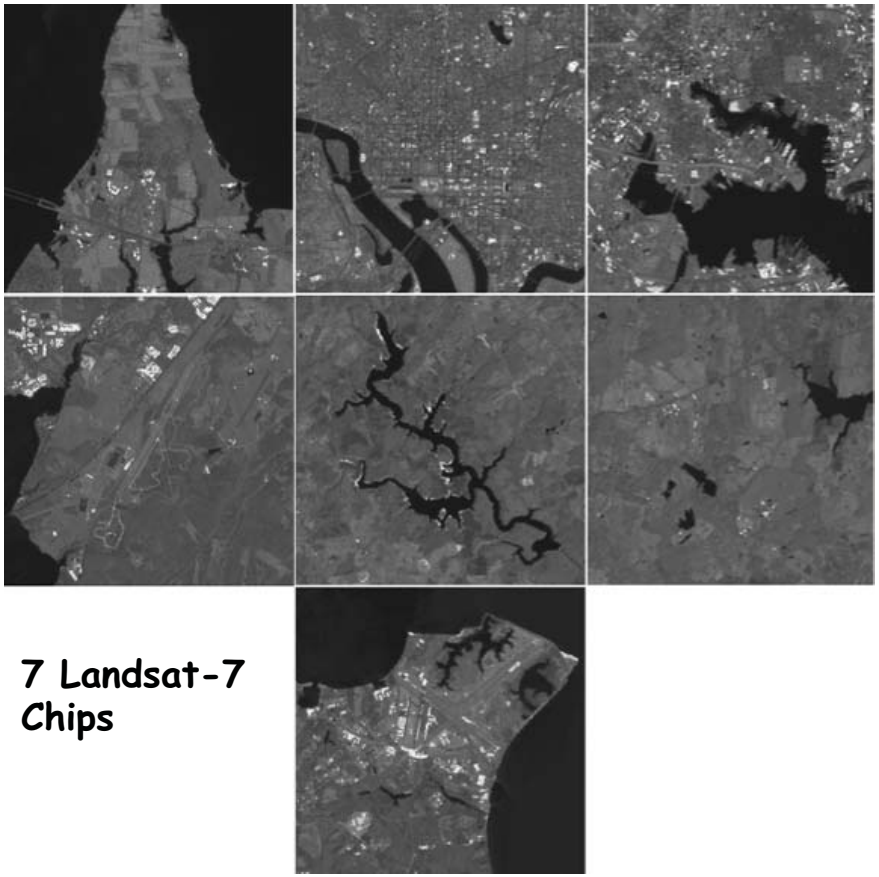

7 Landsat-7 Chips

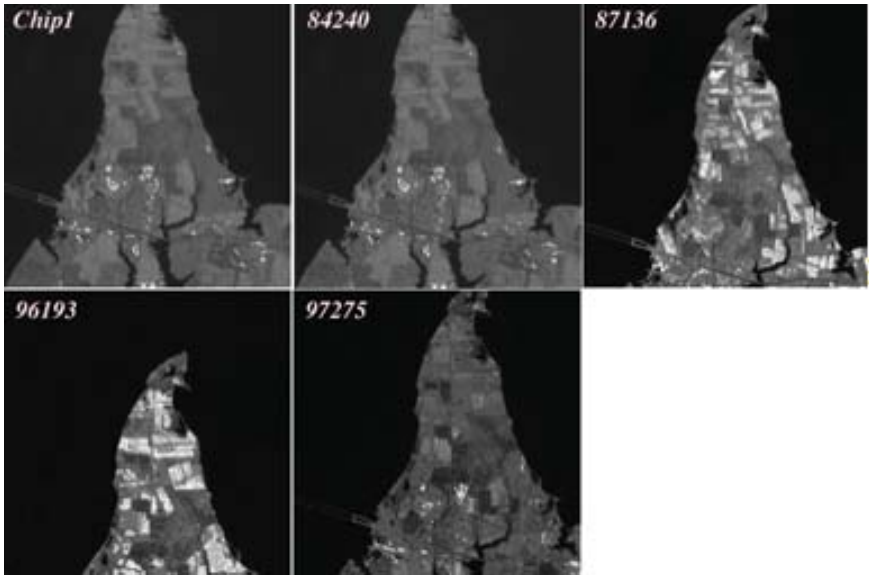

One chip and 4 Corresponding Windows Extracted from 4 Multi-Temporal Landsat Imagery

Algorithm Testing Using …
Landsat-TM Multitemporal Data (3)

Chip #	84240	87136	96193	97275
#1 - Rot:	0	0	1	0
TX	8	18	12	21
TY	-39	-25	-92	-28
Distance	0.00	1.00	1.80	0.00
#2 - Rot:	0	-0.5	1	0
TX	8	11	-66	22
TY	-41	-41	4	-30
Distance	0.00	0.62	1.93	0.00
#3 - Rot:	0	-0.5	-0.3	0
TX	8	11	10.84	21
TY	-40	-41	-96	-29
Distance	1.00	0.89	0.52	0.00
#4 - Rot:	0	0.8	0	0
TX	8	12.34	11	21
TY	-41	--38.12	-94	-28
Distance	1.00	0.96	0.00	0.00
#5 - Rot:	0.4	0.7	0	0
TX	7.8	10.4	-38	20
TY	-40.86	--40.34	52	-31
Distance	0.94	0.93	2.24	0.00
#6 - Rot:	0	-0.8	0.3	0
TX	6	10.61	11.5	22
TY	-41	-41.94	-99	-33
Distance	1.00	0.78	0.70	0.00
#7 - Rot:	0.5	0	0	0
TX	9	12	12	22
TY	-40	-38	-94	-29
Distance	0.56	0.00	0.00	0.00

Transf.	84240	87136	96193	97275
Rotation	0.013	0.003	-0.042	-0.143
Transl-x	7.18	11.43	12.61	21.20
Transl-y	-41.12	-40.49	-95.38	-28.85

Global Registration for 4 Scenes

Transf.	84240	87136	96193	97275
Rotation	0.00	0.00	0.00	0.00
Transl-x	7.18	10.55	9.48	20.97
Transl-y	-40.06	-39.16	-95.16	-28.97

Manual Registration for 4 Scenes

- This Chesapeake Bay Example:
  Global Accuracy Error ≈ 0.82 pixel
- Other Virginia Scenes:
  Global Accuracy Error ≈ 0.31 pixel

Algorithm Testing Using …
EO-1 and Global Land Survey (GLS) Maps

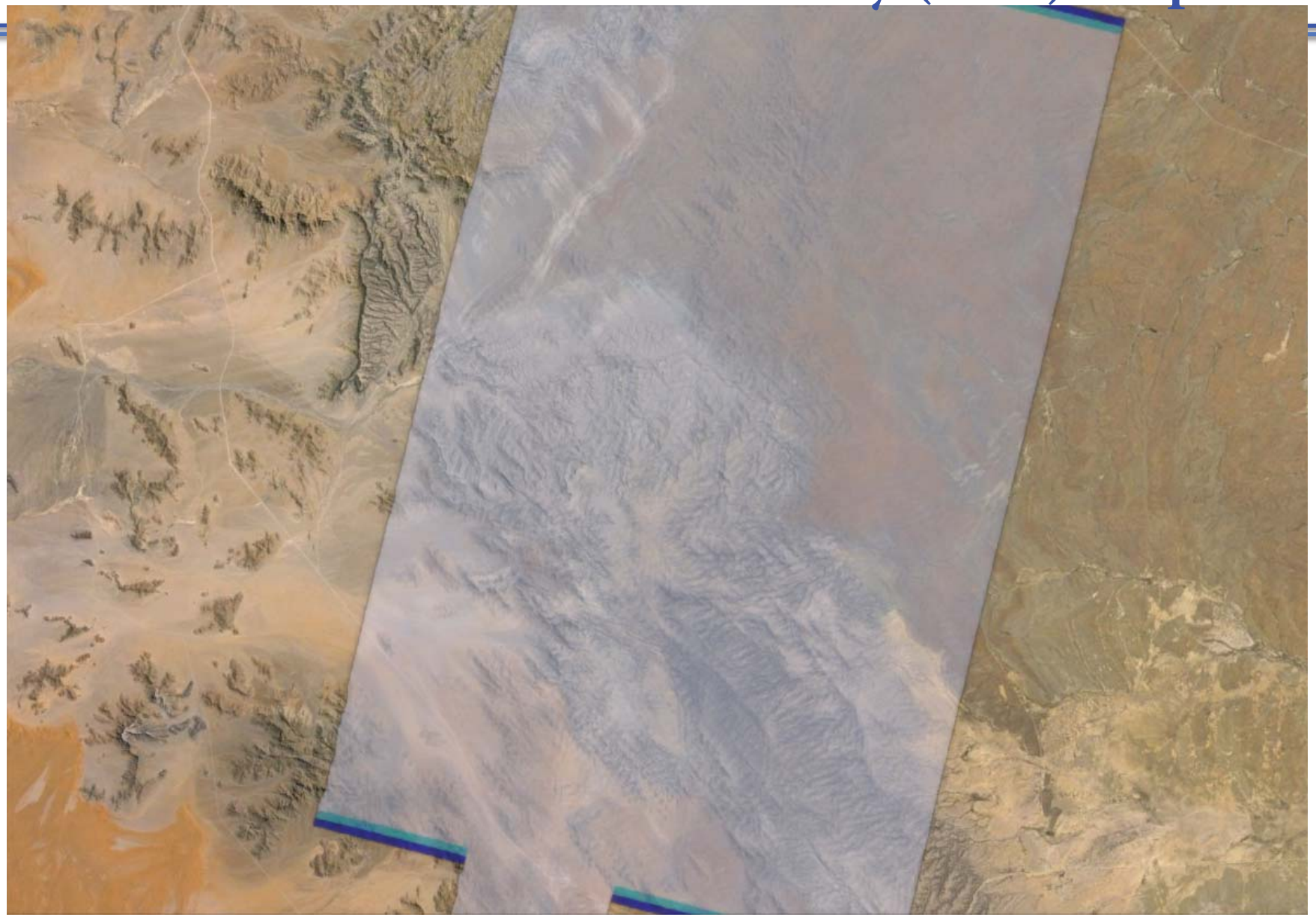

Algorithm Testing Using …
EO-1 and Global Land Survey (GLS) Maps (2)

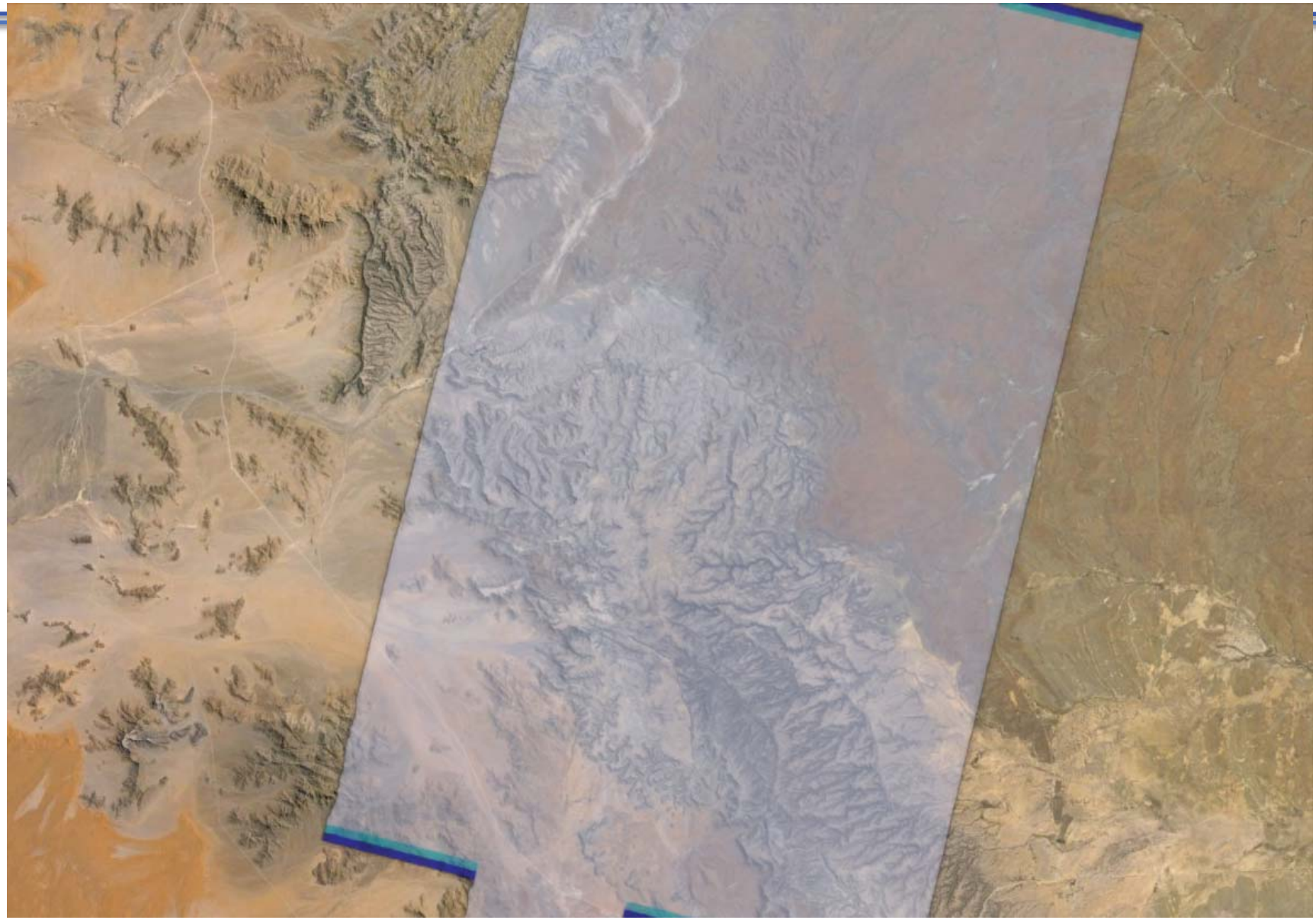

Algorithm Testing Using … Multisensor Data

- Multi-Sensor Data
  - EOS Validation Core Sites
  - IKONOS/Landsat-7/MODIS/ SeaWiFS
    - **Red and NIR** bands for each sensor
    - **Spatial resolutions**: IKONOS: 4m; ETM+: 30m; MODIS: 500m; SeaWiFS: 1000m
  - 4 different sites:
    - **Coastal Area:** VA, Coast Reserve Area, October 2001
    - **Agriculture Area**: Konza Prairie in State of Kansas, July to August 2001
    - **Mountainous Area**: Cascades Site, September 2000
    - **Urban Area**: USDA Site, Greenbelt, MD, May 2001

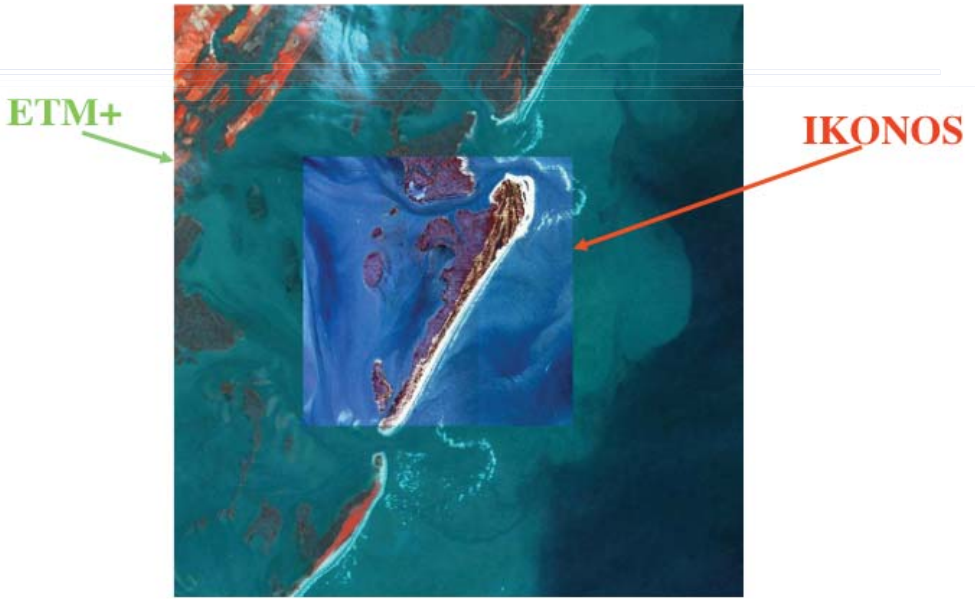

ETM/IKONOS - Coastal VA Data

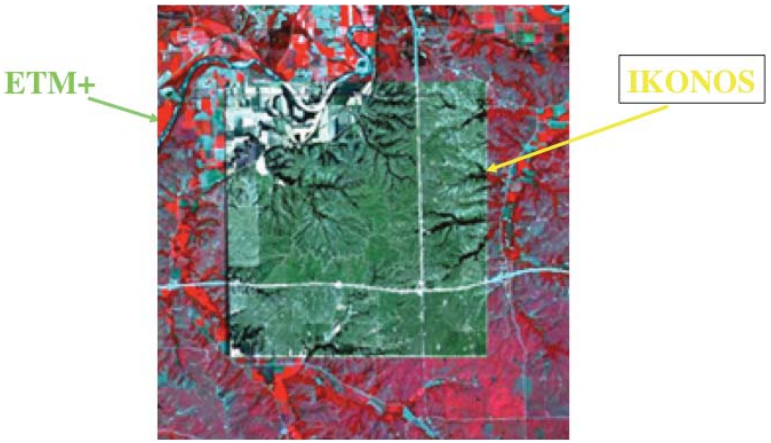

ETM/IKONOS - Agricultural Konza Data

Algorithm Testing Using …
EOS Validation Core Sites (2)

Pair to Register	Method 1 (GC)		Method 2 (GGD)		Method 3 (WCE)		Method 4 (WMIE)		Method 5 (WHR)	
	Rotation	Translation	Rotation	Translation	Rotation	Translation	Rotation	Translation	Rotation	Translation
(1) etm_nir_31.25.power / etm_red_31.25.extract	Rotation = 0 , Translation = (0,0) computed by all methods, using seven sub-windows pairs									
(2) iko_nir_3.91.power / etm_nir_31.25.extract	_	(2,1)	0.0001	(1.9871,-0.0564)	0	(2,0)	0	(2,0)	0	(0,0)
(3) iko_red_3.91.power / etm_red_31.25.extract	_	(2,1)	-0.0015	(1.7233,0.2761)	0	(2,0)	0	(2,0)	0	(0,0)
(4) etm_nir_31.25.power / modis_day249_cc_nir.extract	_	(-2,-4)	0.0033	(-1,7752,-3.9238)	0	(-2,-4)	0	(-2,-4)	0	(-3,-3.5)
(5) etm_red_31.25.power / modis_day249_cc_red.extract	_	(-2,-4)	0.0016	(-1.9665,-3.9038)	0	(-2,-4)	0	(-2,-4)	0	(-2,-3.5)
(6) modis_day249_cc_nir.power / seawifs_day256_to249_nir.extract	_	(-9,0)	0.0032	(-8.1700,0.2651)	0	(-8,0)	0	(-9,0)	0.5	(-6,2)
(7) modis_day249_cc_red.power / seawifs_day256_to249_red.extract	_	(-9,0)	0.0104	(-7.6099,0.5721)	0	(-8,0)	0	(-8,0)	0.25	(-7,1)

- GC: Gray Levels + Fast Fourier Correlation
- GGDL Gray Levels + Gradient Descent
- WCE: Wavelets + Correlation
- WMIE: Wavelets + Mutual Information
- WHR: Wavelets + Hausdorff + Robust Feature Matching

Algorithm Testing Using …
EOS Validation Core Sites (3)

Image Name	Computed X	Computed Y	Comes from Registered Pair
IKONOS red	0	0	(Starting Point)
IKONOS nir	-0.2500	-0.2500	IKO red to ETM red and ETM red to IKO nir
IKONOS nir	-0.2500	-0.3125	IKO red to ETN nir and ETM nir to IKO nir

Table 3 - *Self-Consistency Study of the Normalized Correlation Results*

Image Name	Computed X	Computed Y	Comes from Registered Pair
IKONOS red	0	0	(Starting Point)
IKONOS nir	0.2500	0.0000	IKO red to ETM red and ETM red to IKO nir
IKONOS nir	0.1250	-0.1250	IKO red to ETN nir and ETM nir to IKO nir

Table 4 - *Self-Consistency Study of the Mutual Information Results*

These consistency studies show between 0.125 and 0.25 pixel errors using circular registrations of IKONOS NIR and Red data

References …

- J. Le Moigne, 1994, "Parallel Registration of Multi-Sensor Remotely Sensed Imagery Using Wavelet Coefficients," SPIE's OE/Aerospace Sensing, Wavelet Applications Conference, Orlando, April 5-8, 432-443.
- J. Le Moigne, W. Xia, J.C. Tilton, B-T. Lerner, E. Kaymaz, J. Pierce, S. Raghavan, S. Chettri, T. El-Ghazawi, M. Manohar, N. Netanyahu, W. Campbell, and R. Cromp, 1997, " Towards an Intercomparison of Automated Registration Algorithms for Multiple Source Remote Sensing Data" *Image Registration Workshop,* NASA Goddard Space Flight Center, November 20-21, 1997, NASA Publication #CP-1998-206853.
- H.S. Stone, J. Le Moigne, and M. McGuire, 1999, "Image Registration Using Wavelet Techniques," *IEEE Transactions on Pattern Analysis and Machine Intelligence*, *PAMI,* Vol. 21, No.10, October 1999.
- N. Netanyahu, J. Le Moigne and J. Masek, 2004, "Geo-Registration of Landsat Data by Robust Matching of Wavelet Features," *IEEE Transactions on Geoscience and Remote Sensing*, Volume 42, No. 7, pp. 1586-1600, July 2004.
- J. Le Moigne, H. Stone, A. Cole-Rhodes, R. Eastman, P. Jain, K. Johnson, J. Morisette, N. Netanyahu, and I. Zavorin, 2004 "A Study of the Sensitivity of Automatic Image Registration Algorithms to Initial Conditions," 2004 IEEE International Geoscience and Remote Sensing Symposium, IGARSS'04, Anchorage, Alaska, September 20-24, 2004.
- I. Zavorin, and J. Le Moigne, 2005, "Use of Multiresolution Wavelet Feature Pyramids for Automatic Registration of Multisensor Imagery," *IEEE Transactions on Image Processing*, Vol. 14, No. 6, pp. 770-782, June 2005.
- J. Le Moigne, A. Cole-Rhodes, R. Eastman, P. Jain, A. Joshua, N. Memarsadeghi, D. Mount, N. Netanyahu, J. Morisette, E. Uko-Ozoro, 2006, "Image Registration and Fusion Studies for the Integration of Multiple Remote Sensing Data," Proceedings of the 2006 IEEE International Conference on Acoustics, Speech and Signal Processing, Toulouse, France, May 14-19, 2006.

Section 2f
Fusion using cokriging

Kriging and Cokriging …

- Kriging and cokriging are geostatistical techniques used for interpolation purposes, originally used in geo-statistics, mining, and petroleum engineering applications
- Both methods are generalized forms of univariate and multivariate linear regression models:
  - They are linear-weighted averaging methods, similar to other interpolation methods
  - Other methods use weights based on the distance of each control point (sample value) from the target location; controls points closer to the target receive the larger weights => not necessarily true if the data exhibit strong anisotropy

Kriging and Cokriging (2)

- Kriging and cokriging
  - Pioneered by Danie Krige, 1951; formalized by Georges Matheron in the 1960s
  - Ability to capture anisotropy of the underlying variables through the spatial covariance model:
    - Distant control points along the axis of maximum correlation should have greater influence on the interpolated value
    - Weights depend not only on distance, but also on the direction and orientation of the neighboring data to the unsampled
- Generalized version of *kriging (B.L.U.E):*
  - *Best:* aims to minimize variance of the errors
  - *Linear:* estimates are weighted linear combination of the available data
  - *Unbiased:* tries to have mean residual, or error, equal to zero.
  - *Estimator:* $\widehat{v} = \sum_{j=1}^{n} w_j . v$

Cokriging …

Interpolation using more that one type of variable to estimate an unknown value at a particular location.

$$\hat{u}_0 = \sum_{i=1}^{n} a_i.u_i + \sum_{j=1}^{m} b_j.v_j$$

Estimation error:

$$R = \hat{U}_0 - U_0 = w^t Z,$$

$$w^t = (a_1,\ldots,a_n,b_1,\ldots,b_m,-1)$$

$$Z^t = (U_1,\ldots,U_n,V_1,\ldots,V_m,U_0)$$

Goal of cokriging is to *minimize variance of error* subject to some constraints (to ensure unbiasedness of our estimate, here "ordinary cokriging")

$$Var(R) = w^t C_z w$$

$$\sum_{i=1}^{n} a_i = 1, \sum_{j=1}^{m} b_j = 0$$

Cokriging (2)

- Variance to minimize with 2 constraints:

$$Var(R) = w^t C_z w$$

$$= \sum_i^n \sum_j^n a_i a_j Cov(U_i U_j) + \sum_i^m \sum_j^m b_i b_j Cov(V_i V_j)$$

$$+ 2\sum_i^n \sum_j^m a_i b_j Cov(U_i V_j) - 2\sum_i^n a_i Cov(U_i U_0)$$

$$- 2\sum_j^m b_j Cov(V_j U_0) + Cov(U_0 U_0).$$

$$Var(R) = w^t C_z w + 2\mu_1 \left(\sum_{i=1}^n a_i - 1 \right) + 2\mu_2 \left(\sum_{j=1}^m b_j \right).$$

Where m1 and m2 are 2 Lagrange multipliers

Cokriging (3)

- The next step is taking partial derivatives of the above equation with respect to all n + m cokriging variables and the two Lagrange multipliers and setting them to zero. Then, we have the following n+m+2 equations to solve:

$$\sum_{i=1}^{n} a_i Cov(U_i U_j) + \sum_{i=1}^{m} b_i Cov(V_i U_j) + \mu_1 = Cov(U_0 U_j), \quad \text{for (j = 1…n)}$$

$$\sum_{i=1}^{n} a_i Cov(U_i V_j) + \sum_{i=1}^{m} b_i Cov(V_i V_j) + \mu_2 = Cov(U_0 V_j), \quad \text{for (j = 1…m)}$$

$$with \sum_{i=1}^{n} a_i = 1$$

$$and \sum_{j=1}^{m} b_j = 0$$

Experiments Cokriging – Spectral Dimension

- Spectral dimension
  - ALI: 9 multispectral bands
  - Hyperion: 220 hyperspectral bands
  - Increase spectral resolution of ALI where needed using Hyperion information
- One variable only
- Software used
  - UCL-FAO Agromet project

    (http://www.aigeostats.org/software/Geostats_software/agromet.htm)
  - C++

Results Cokriging – Spectral Dimension

Original 1 pixel plot for ALI and Hyperion

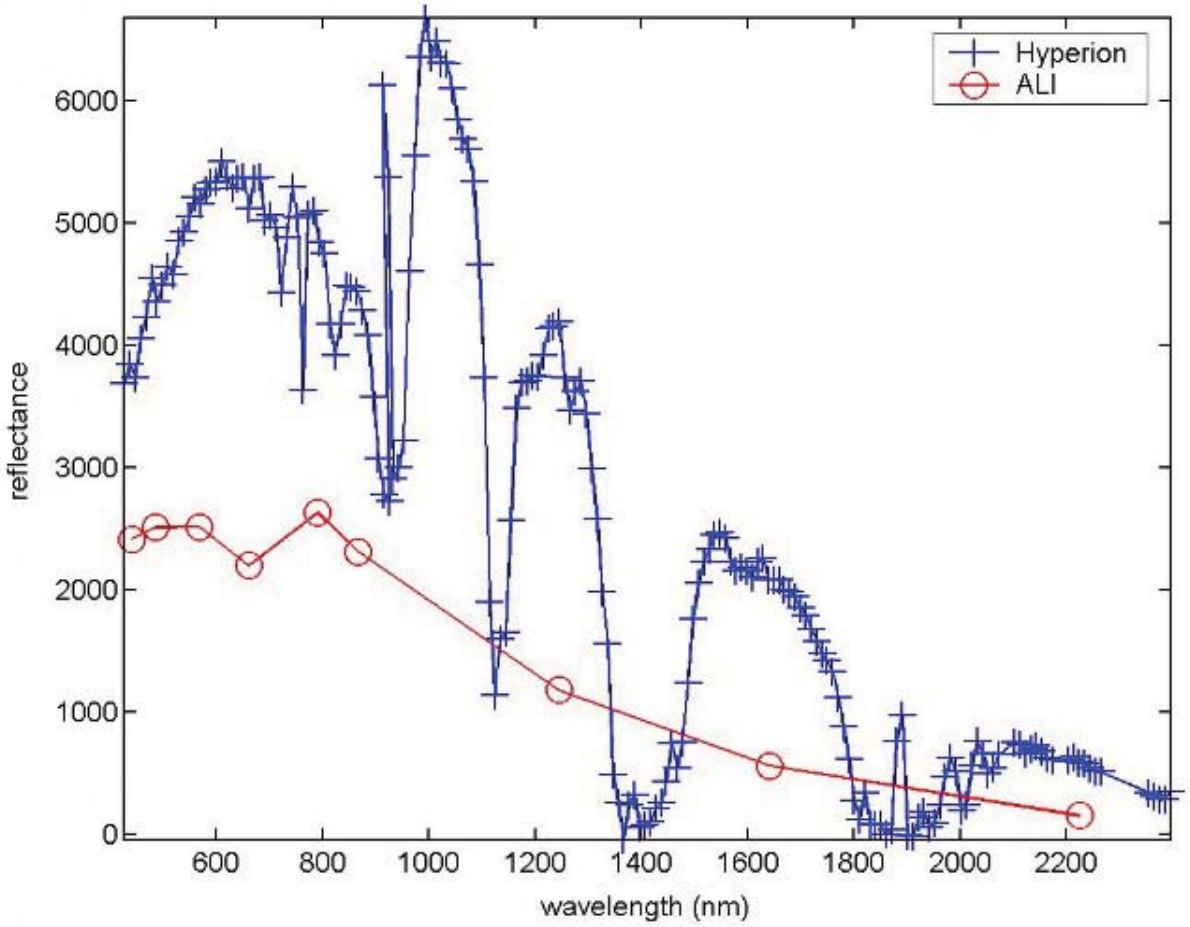

Results Cokriging – Spectral Dimension (2)

Fusion results on one pixel using cokriging by creating one band/value in center of each wavelength interval where ALI data is missing.

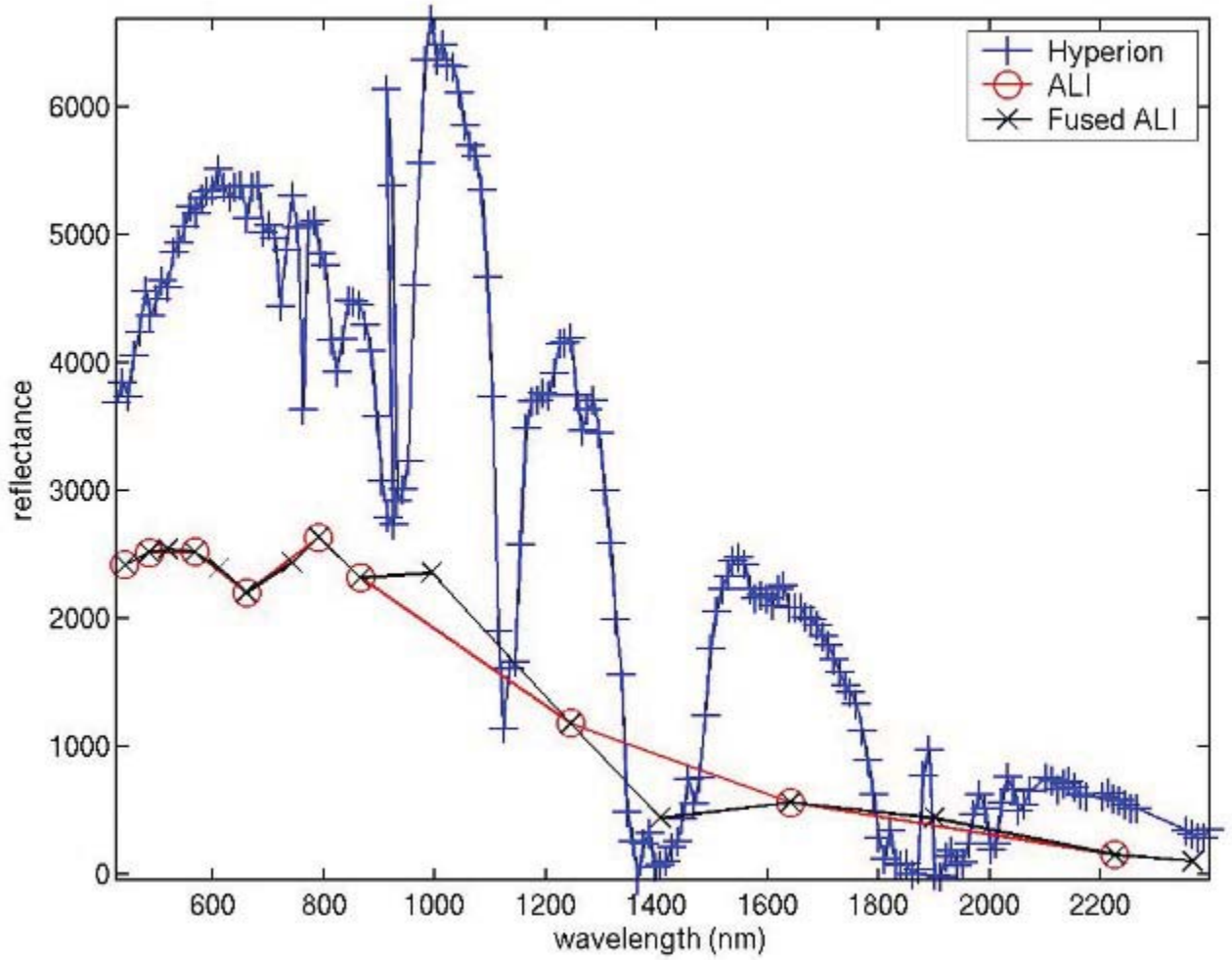

Results Cokriging – Spectral Dimension (3)

Fusion results on one pixel using cokriging by estimating up to 3 values in each wavelength interval where ALI data is missing.

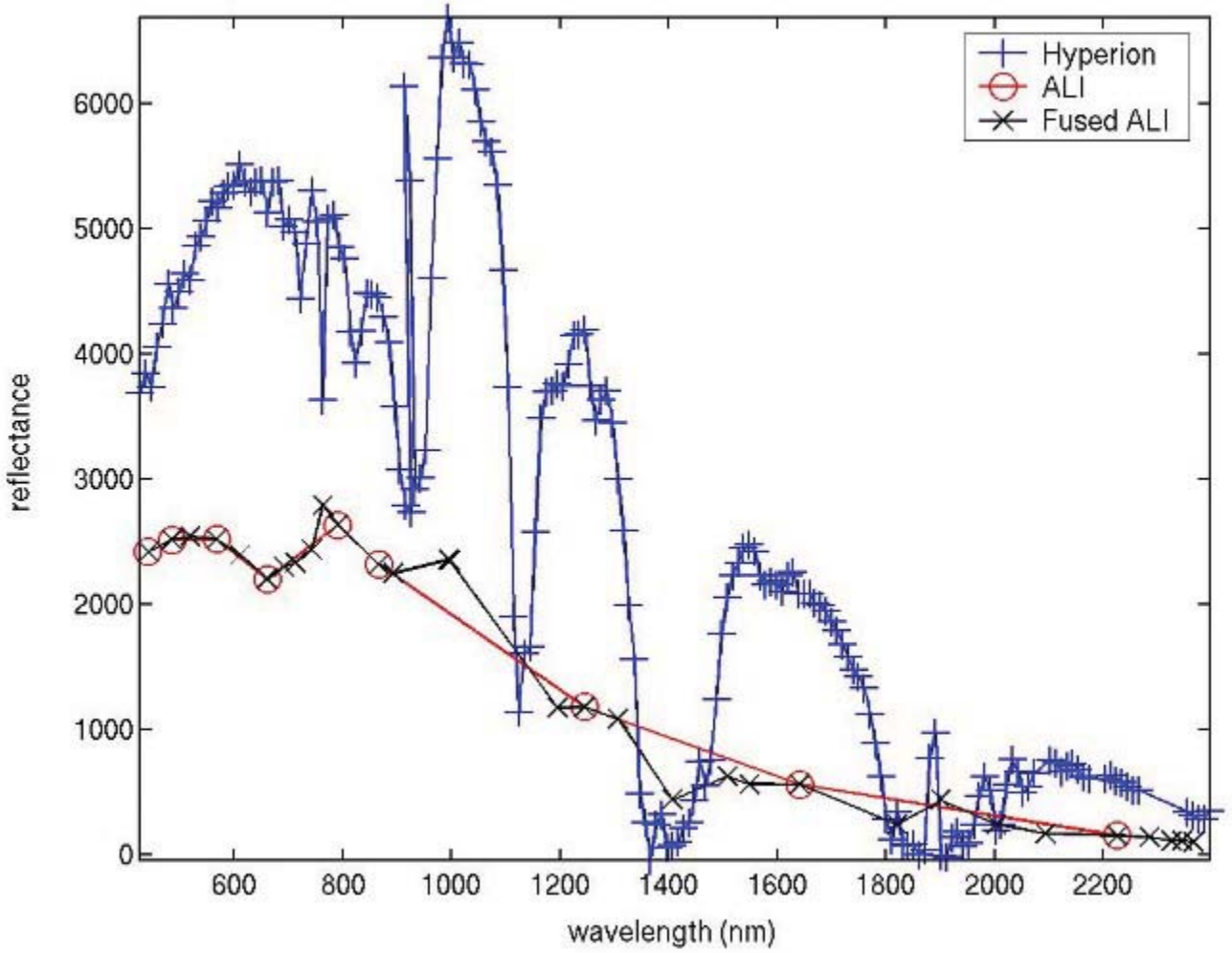

Results Cokriging – Spectral Dimension (4)

Fusion results on one pixel using cokriging by estimating values at all Hyperion centers in each wavelength interval where ALI data is missing.

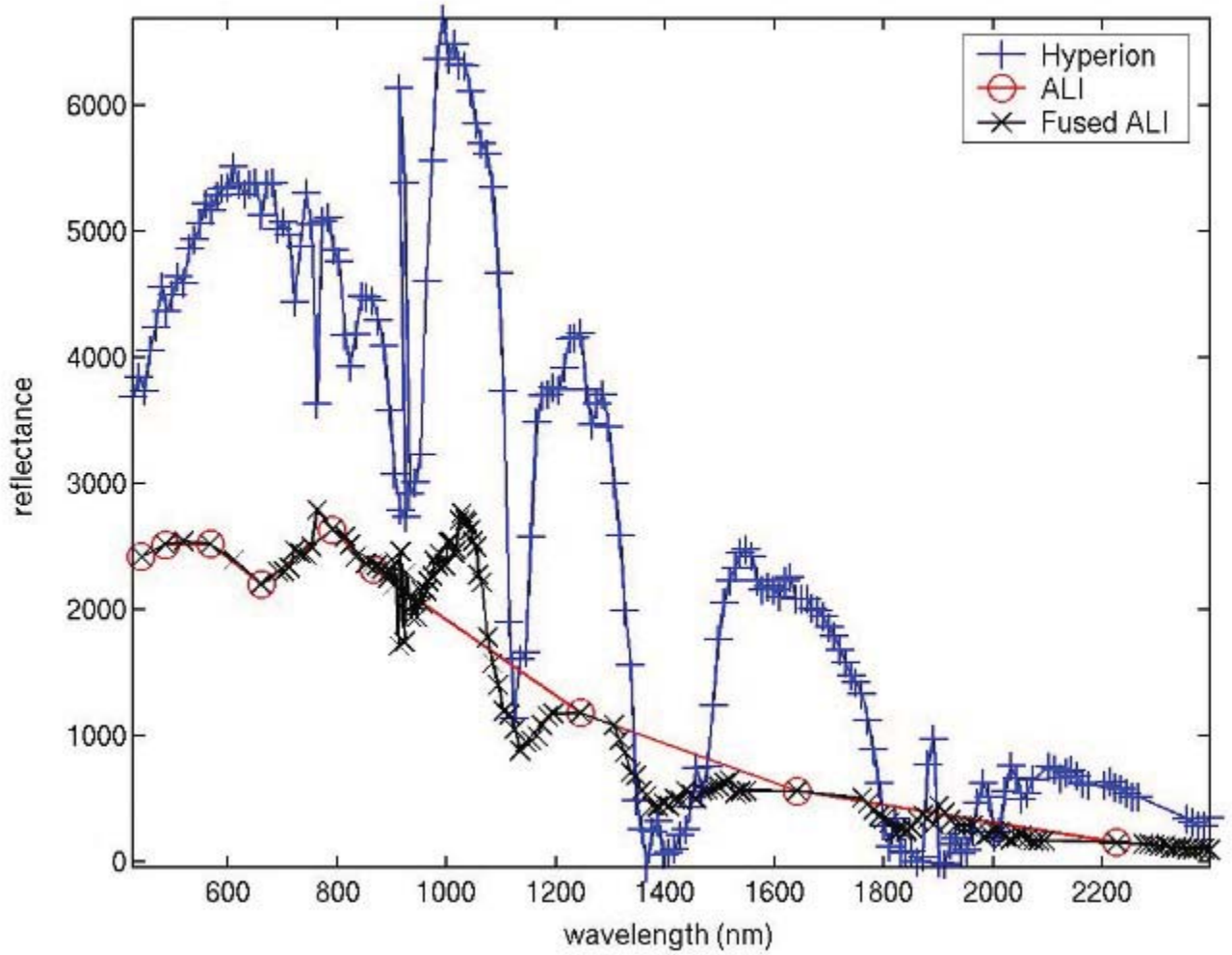

Experiments Cokriging – Fusion of Panchromatic and Multispectral

- Landsat 7 ETM data sets
  - Datasets provided by IEEE Data Fusion Committee
  - 8 Bands:
    - 7 multispectral at 30 m spatial resolution
    - 1 panchromatic at 15 m spatial resolution
- Objective
  - Pan sharpening of selected multispectral bands
- Comparative Methods
  - Cokriging
  - PCA
  - Wavelets

Experiments Cokriging – Fusion of Panchromatic and Multispectral (2)

Landsat 7 Multispectral Bands 2, 3, and 4

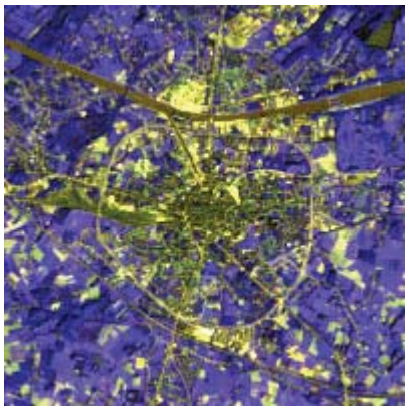

Landsat Panchromatic Band 8

Band	Resolution	
	Spatial (meters)	Spectral *(m)*
1	30	0.45–0.52
2	30	0.53–0.61
3	30	0.63–0.69
4	30	0.78–0.90
5	30	1.55–1.75
6	30	10.4–12.5
7	30	2.09–2.35
8 (PAN)	15	0.52–0.90

Methods: Cokriging – Fusion of Panchromatic and Multispectral

Spectral Resolution

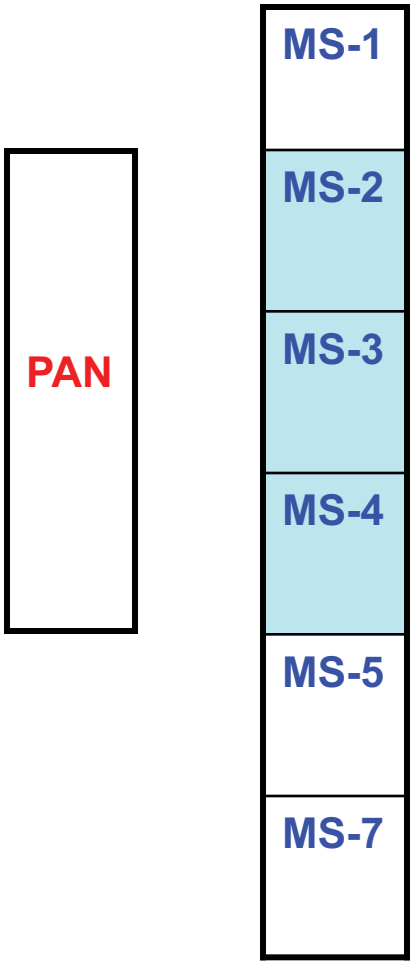

Pan + MS-2 ⇨ fused_b2
Pan + MS-3 ⇨ fused_b3
Pan + MS-4 ⇨ fused_b4

Spectral Resolution
1 pixel of MS band

MS-Value

Pan Value 1	Pan Value 2
Pan Value 3	Pan Value 4

x1 y1 p1 ?
x2 y2 p2 ?
x3 y3 p3 ms
x4 y4 p4 ?
(using nearest Neighborhs, e.g. 5x5)

Methods: Principal Components Analysis – Fusion of Panchromatic and Multispectral

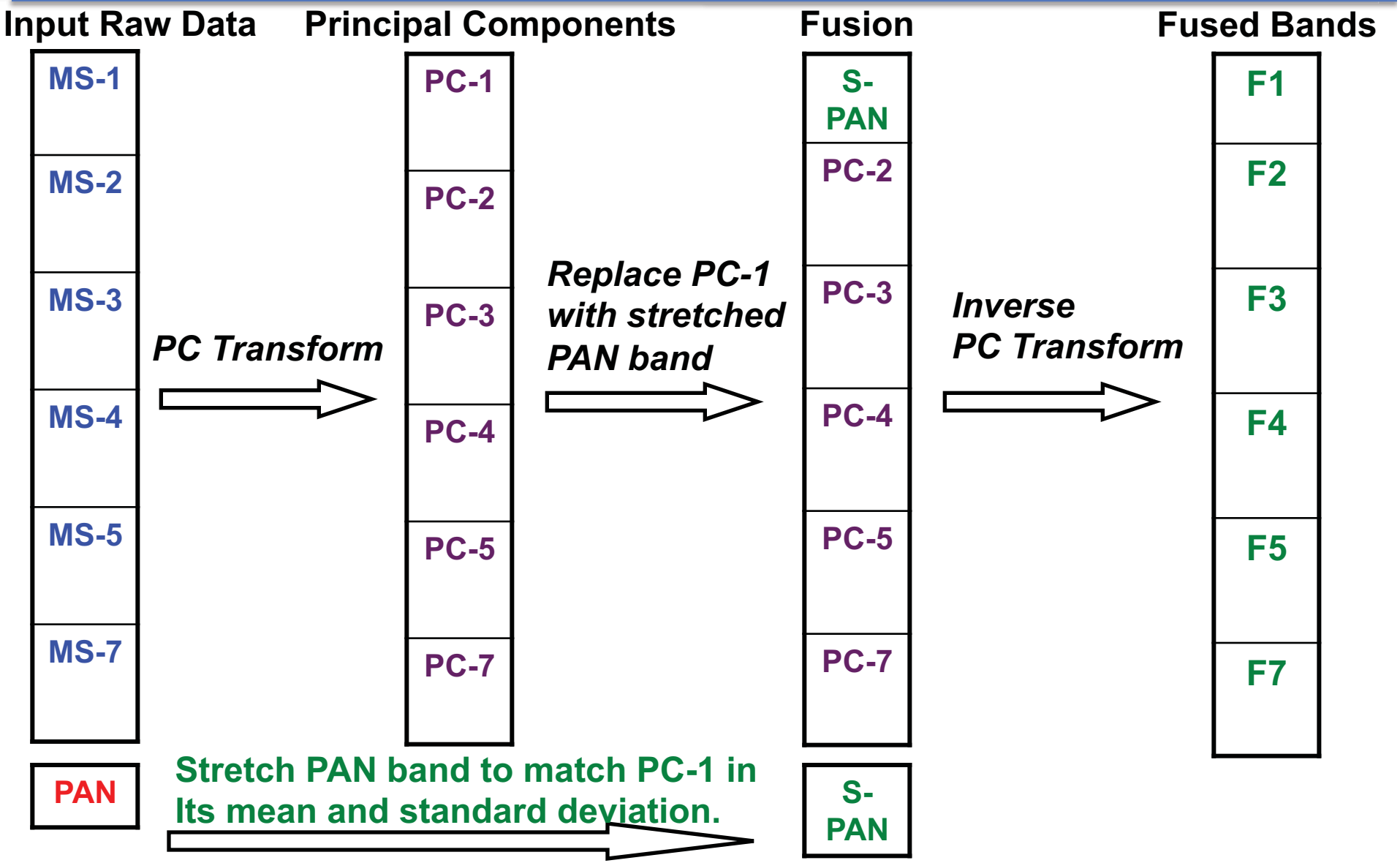

Methods: Wavelet-Based Fusion – Fusion of Panchromatic and Multispectral

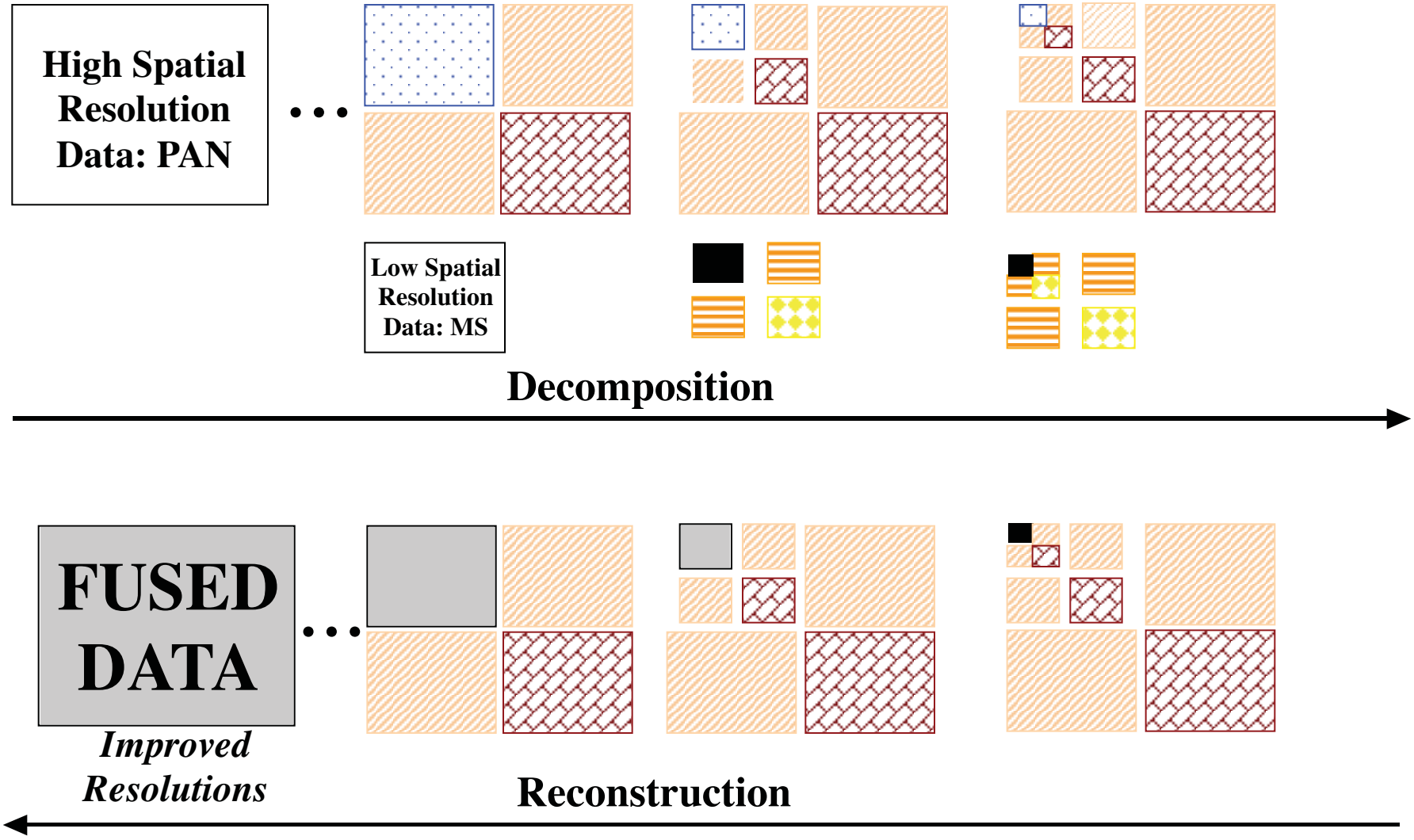

Evaluation Fusion Results – Fusion of Panchromatic and Multispectral

- Past Quality Metrics
  - Piella, etc.
  - Gray level only
  - No support for multi-spectral image
- Objective
  - Improved Classification
    - Performed k-means with k=7, max iterations 15 (for PCA and wavelets)
  - Needs ground truth
- Similarities
  - Spatial Quality: Entropy
  - Spectral quality: correlation
- Differences
  - Added Texture
  - Co-occurrence matrix for statistical texture properties (Haralick,1973)
  - Variance image

Results Cokriging – Fusion of Panchromatic and Multispectral

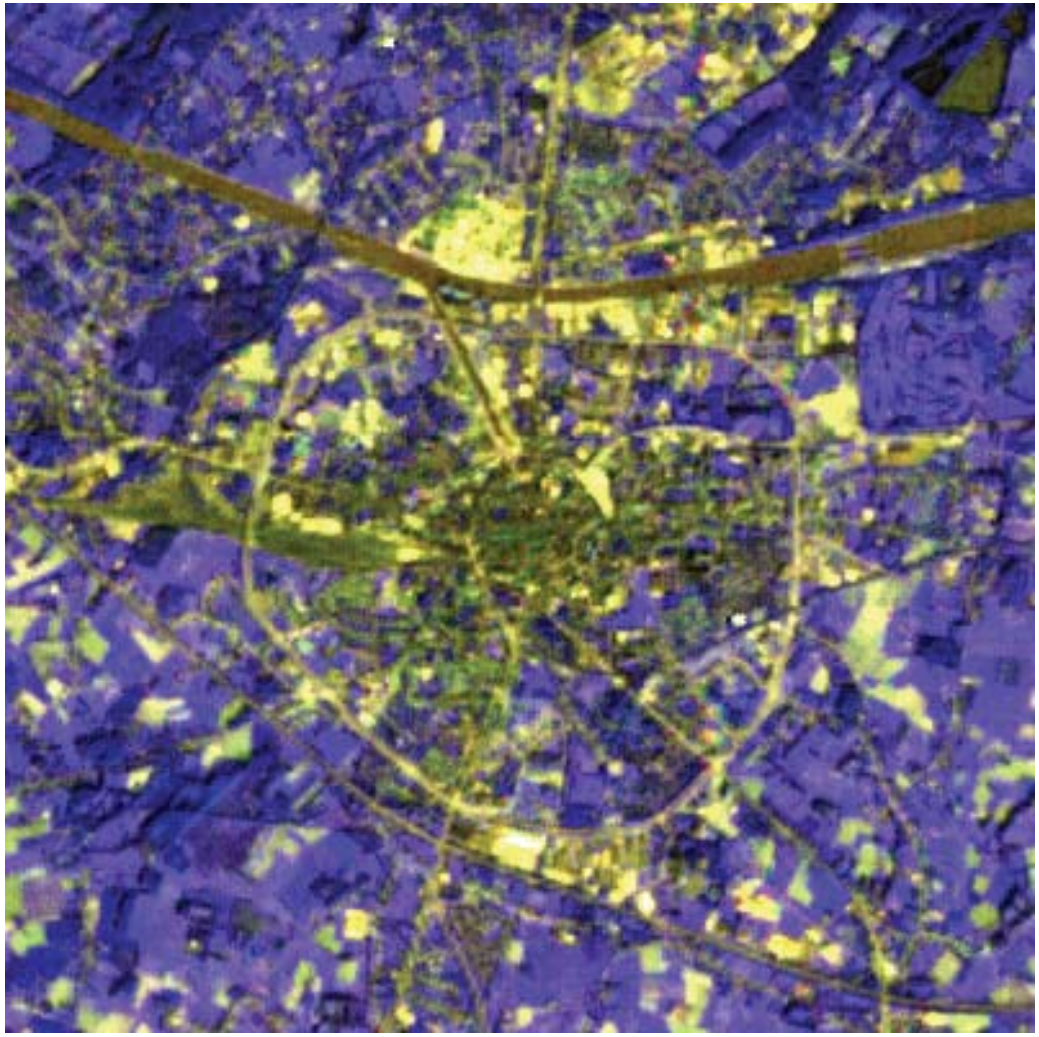

Landsat Pan-sharpened MS bands 2, 3, and 4
***Through* Cokriging with Pan band 8**

Results PCA and Wavelets – Fusion of Panchromatic and Multispectral

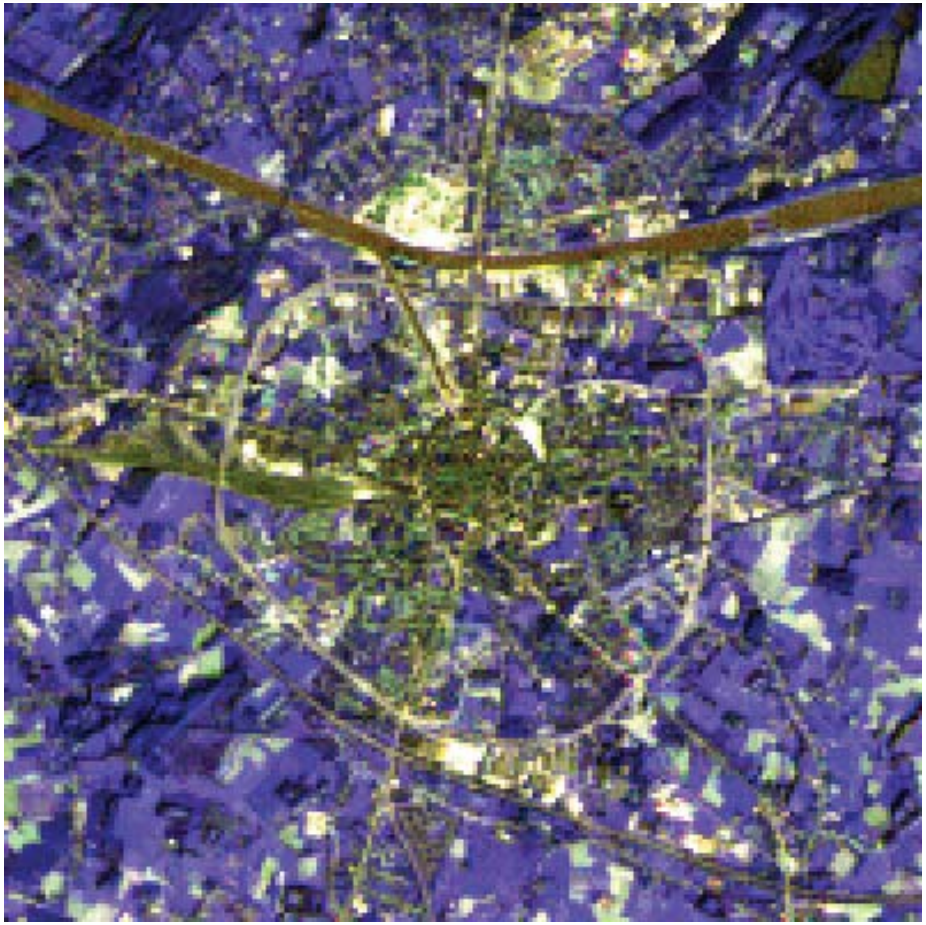

Through PCA

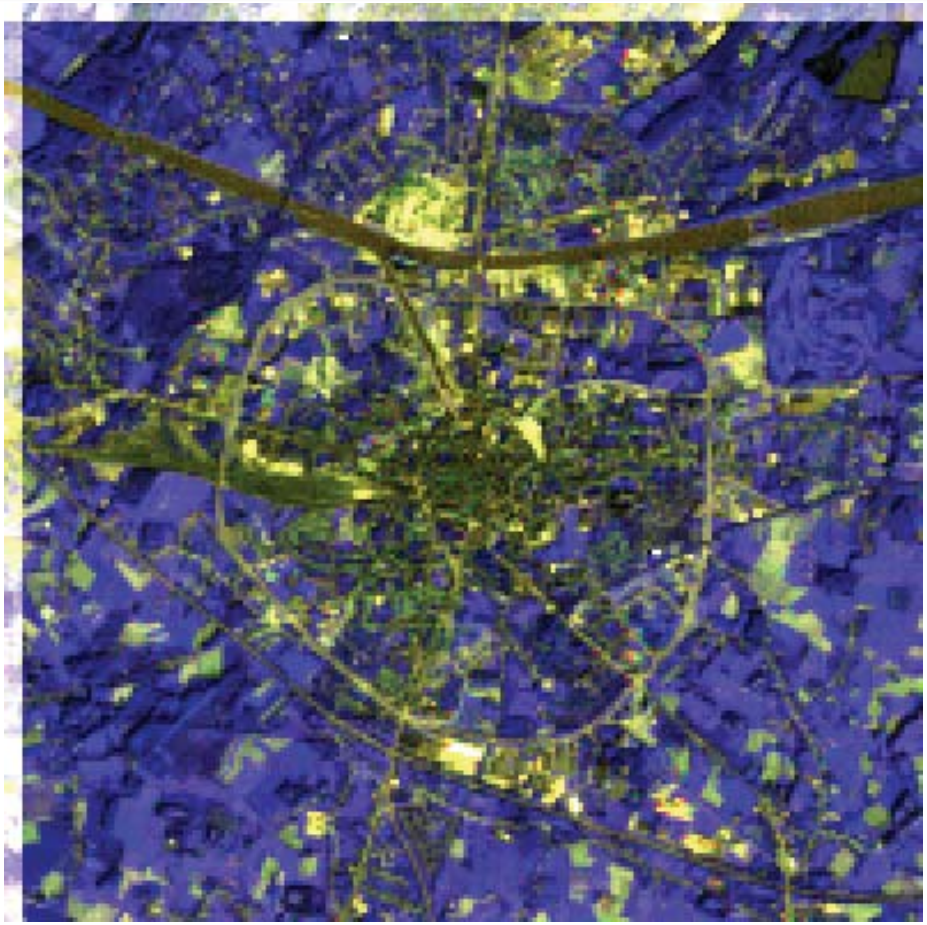

Through Wavelets

Landsat Pan-sharpened MS bands 2, 3, and 4 with Pan band 8

Results Evaluation though Correlation – Fusion of Panchromatic and Multispectral

Wavelet	PCA	Cokriging
• Fuse pair of bands at a time • Require various spatial resolution to differ by power of 2	• Fuse multiple bands at a time • Require the same number of pixels (same image dimension) for all bands	• Fuse multiple bands at a time • Fuse data with different spatial and spectral resolutions • Fuse data of different natures • Can handle scattered data

CORRELATION OF FUSED BANDS WITH MS INPUT BANDS

Bands	Wavelet	PCA	Cokriging
f2, b2	0.82	0.99	0.91
f3, b3	0.84	0.99	0.93
f4, b4	0.92	0.75	0.93
Average	0.86	0.91	0.92

Results Evaluation though Entropy – Fusion of Panchromatic and Multispectral

ENTROPY OF MS AND FUSED BANDS

Original Bands		Fused Bands	Wavelet	PCA	Cokriging
b2	2.68	f2	3.12	2.69	3.23
b3	3.01	f3	3.28	3.72	3.64
b4	3.44	f4	3.93	5.21	4.90
Average	3.04		3.44	3.87	3.92

Results Evaluation though Co-Occurrence Matrix – Fusion of Panchromatic and Multispectral

MEAN ENTROPY OF ENTROPY IMAGES OBTAINED THROUGH CO-OCCURRENCE MATRICES

Original Bands		Fused Bands	Wavelet	PCA	Cokriging
b2	1.37	f2	1.37	1.37	1.44
b3	1.42	f3	1.45	1.49	1.45
b4	1.77	f4	1.78	2.02	1.96
Average	1.52		1.53	1.63	1.62

References …

- D.G. Krige, A statistical approach to some mine valuations and allied problems at the Witwatersrand, Master's thesis of the University of Witwatersrand, 1951.
- G. Matheron, "Principles of geostatistics", Economic Geology, 58, pp 1246–1266, 1963
- J. Le Moigne, 2004, “Registration and Fusion of Multiple Source Remotely Sensed Image Data,” Invited Talk at the 2004 American Geophysical Union (AGU) Fall Meeting, Data and Services for Space and Earth Sciences Session, San Francisco, December 13-17, 2004.
- A. Agarwal, T. El-Ghazawi, and J. Le Moigne, 2005, “Enhancing Dust Storm Detection Using PCA-Based Data Fusion,” Proceedings of 2005 IEEE International Geoscience and Remote Sensing Symposium, IGARSS'05, Seoul, Korea, July 25-29, 2005.
- N. Memarsadeghi, J. Le Moigne, D. Mount, and J. Morisette, 2005, “A New Approach to Image Fusion Based on Cokriging,” FUSION'2005, 8th International Conference on Information Fusion, Philadelphia, Pennsylvania, July 25-28, 2005, Volume 1, pages 622-629.
- J. Le Moigne, A. Cole-Rhodes, R. Eastman, P. Jain, A. Joshua, N. Memarsadeghi, D. Mount, N. Netanyahu, J. Morisette, E. Uko-Ozoro, 2006, “Image Registration and Fusion Studies for the Integration of Multiple Remote Sensing Data,” Proceedings of the 2006 IEEE International Conference on Acoustics, Speech and Signal Processing, Toulouse, France, May 14-19, 2006.
- N. Memarsadeghi, J. Le Moigne, and D. Mount, 2006, “Image Fusion Using Cokriging,” 2006 IEEE International Geoscience and Remote Sensing Symposium, IGARSS'06, Denver, CO, July 2006.